

Convergence of subdivision sequences of discrete surfaces

著者	Tao Chen
学位授与機関	Tohoku University
URL	http://hdl.handle.net/10097/00126067

博 士 論 文

CONVERGENCE OF SUBDIVISION
SEQUENCES OF DISCRETE
SURFACES

陶 辰

令和元年

DISSERTATION

CONVERGENCE OF SUBDIVISION
SEQUENCES OF DISCRETE
SURFACES

Submitted by
Tao Chen
Mathematical Institute
Graduate School of Science

In partial fulfillment of the requirements
For the Degree of Doctor of Philosophy
Tohoku University
Sendai, Japan

Aug 2019

ACKNOWLEDGEMENT

My deepest gratitude goes first and foremost to Prof. Kontani Motoko, my supervisor, for her constant encouragement and guidance. She provides fertile ground on which this thesis could grow. Five years ago, Prof. Kontani gave me a chance so that I can start this wonderful and amazing journey in the world of mathematics. As a supervisor, Prof. Kotani does not only teach me mathematics, but how to think in mathematics, how to work in mathematics, and how to express in mathematics. As a friend, Prof. Kotani gave me a lot of experience on the daily life when I first stepped into this country. She is always there with the patient and encouraging smile on her face and discussing my naive ideas.

Second, I would like to express my heartfelt gratitude to Prof. Naito Hisashi from Nagoya University, who gave me a lot of advice on the thesis, especially the numerous discussions which tremendously help me to understand the limit space of the subdivision sequences. He spends a lot of time in listening to my ideas and providing critically remarks on many aspects of this work.

Also, I am grateful to several people for their encouragement and for many stimulating discussions: Kajigaya Toru, Prof. Tate, Prof. Suito. It is my great pleasure to work with them. Their beautiful and inspirational ways of thinking about geometry encourages me a lot. I also thank Prof. Konrad Polthier and Prof. Ulrich Reitebuch from Freie Universität Berlin, for their inspiring discussions, constructive and critical discussions.

Last but not the least, my thanks would go to my beloved family for their understanding and great confidence in me. Every time in the phone call, my mother tells me not to work so hard and if I feel tired, just go back home, she has prepared all my favorite food. They may know little about my research, but their simple words warms me so that I can stand up and overcome all the problems. In particular, I would like to thank Dr. Wu, for always listening to me and helping me. Her appearance lightens my life. Without her support, I would never go through the difficult time.

Contents

1	Introduction	1
2	Discrete Surfaces	5
2.1	Trivalent graphs in \mathbb{E}^3 and their curvatures	6
2.2	Discrete harmonic and discrete minimal surfaces	8
2.3	Central frame and height function	10
3	The Fundamental Theory of Subdivision	11
3.1	Control net and refinement	11
3.2	Subdivision zoo	13
3.3	Subdivision process	15
3.4	Invariant neighborhood and subdivision matrix	17
3.5	Convergence of subdivisions	18
4	Subdivision Algorithms for Trivalent Graphs in \mathbb{E}^3	22
4.1	Goldberg-Coxeter construction of trivalent graphs	23
4.2	Invariant neighborhood and subdivision matrix	25
4.3	GC-subdivision of discrete surfaces	26
5	Evaluation and estimate	29
5.1	Convergence of the modified subdivision algorithm	29
5.2	The limit set of the subdivision sequence	32
5.3	Monotonicity of the Dirichlet energy	36
6	Numerical Experiments and Applications	38

Chapter 1

Introduction

Modern work on smooth manifolds and surfaces with the Riemannian metric has a long history and belongs to the central theme of the research in differential geometry. However, non-smooth surfaces are also natural mathematical objects and recently get more and more attention. Various topics are considered in this view, such as Metric measure spaces, Polyhedral meshes, Graphs, and Geometric group theory.

Among them, the applications of analysis on discrete objects, in particular, the polyhedral meshes, catch the eye of the society, especially the industry and other scientific fields. For example, U. Pinkall and K. Polthier [24] develop a surface theory on simplicial surfaces with triangulations. They define the mean curvature by using the variational principle of area and energy on each triangular face. They also give a minimization algorithm with conjugation to construct discrete minimal surfaces. In [25], K. Polthier discusses the conforming and non-conforming triangulations and studies their convergence properties. K. Hildebrandt, K. Polthier, and M. Wardetzky [9, 10] generalize the definition of shape operators on a smooth surface and its normal graph and estimate the difference. Another viewpoint comes from A. I. Bobenko and Y. Suris [2, 3]. Their study foci on the discrete isothermic surfaces, namely, conformal quadrilateral meshes and leads to a strong connection between quadrilateral meshes and discrete integrable systems. Furthermore, M. Alexa and M. Wardetzky [1] define a discrete Laplacian on arbitrary polygonal faces by generalizing the cot formula K. Polthier discovered.

Their studies on the polyhedral meshes are based on the motivation of finding a *proper* approximations of a given smooth surface, which produces a large number of applications in the field of computer graphics, engineering design, and animation. However, one may ask a question from an opposite direction, that is, *how to discover a smooth surface from a given discrete object without knowing any information about the underlying surface?*

On the other hand, graph theory studies the combinatorial structures of discrete objects by giving edge relations between isolated vertices. With proper geometric positions, some of the graphs may look like surfaces, still, some are not. For example, the square lattice is appropriate to say a discrete plane with \mathbb{E}^2 as its hidden smooth surface while the cubic lattice cannot be treated as a discrete surface in \mathbb{E}^3 . Hence a natural problem may be asked from this observation, *when does a graph with some geometric descriptions can be treat as a “surface”?*

The initial idea of our work comes from a combination of those two questions, that is, try to identify an underlying surface from a discrete object with graph structures. A

discrete object is usually treated as an abstract set of isolated vertices. By assigning geometric positions and connecting a particular pair of vertices, the discrete object can be seen as a kind of *networks*. The study of M. Kotani, H. Naito and T. Omori in [13] introduces a specific kind of these networks, a trivalent graph in \mathbb{E}^3 , as a discrete surface. In precisely, the discrete surface is defined as a topological trivalent graph realized in \mathbb{E}^3 by a piecewise linear injective. They also define some basic geometric quantities for example, curvatures, by utilizing the trivalent structures. To find the underlying smooth object from a given discrete surface, we use the idea of subdivision algorithms. Generally speaking, the subdivision algorithm is a method that inserts new elements and combinatorial relations into the initial discrete surface. We construct a sequence of discrete surfaces by applying the subdivision algorithm iteratively. If this sequence converged in some certain sense, then we can find the underlying surface as its limit.

Let $\Phi: X \rightarrow \mathbb{E}^3$ with $\mathcal{M} = \Phi(X)$ as a discrete surface, where X is a topological trivalent graph. $\{\mathcal{M}_i\}_{i=0}^\infty$ with $\mathcal{M}_0 = \mathcal{M}$ is a sequence of discrete surfaces constructed by subdivision algorithm. The present thesis includes the following results:

1. By discussing the local Dirichlet energy, we give a proof of the convergence of the subdivision algorithm.

Theorem 5.1.2 ([37]). *The sequence of discrete surfaces $\{\mathcal{M}_i\}_{i=0}^\infty$ that are constructed by the modified GC-subdivisions forms a Cauchy sequence in the Hausdorff topology.*

2. The limit set \mathcal{M}_∞ of this sequence in the Hausdorff topology is divided into three types:

$$\mathcal{M}_\infty = \mathcal{M}_\mathcal{R} \cup \mathcal{M}_\mathcal{V} \cup \mathcal{M}_\mathcal{S}.$$

$\mathcal{M}_\mathcal{R}$ is the set of accumulate vertices of all the rings. $\mathcal{M}_\mathcal{V}$ is the set of all the inserted vertices. $\mathcal{M}_\mathcal{S}$ emerges as a global accumulation. To avoid the third part $\mathcal{M}_\mathcal{S}$, we define the un-branched surface and prove the following theorem

Theorem 5.2.4 ([14]). *Let $\mathcal{M}_0 = \{\mathcal{V}_0, \mathcal{E}_0, \mathcal{R}_0\}$ be a trivalent graph in \mathbb{E}^3 satisfies*

1. *Each edge of \mathcal{M}_0 is shared by two rings at most.*
2. *Any two rings intersect at one edge or empty.*
3. *For any two n -rings \mathbf{r}_i and $\mathbf{r}_j \in \mathcal{R}_0$, the convex hull $\text{conv}(\mathcal{N}(\mathbf{r}_i))$ of the one-neighborhood $\mathcal{N}(\mathbf{r}_i)$ of \mathbf{r}_i and the convex hull $\text{conv}(\mathcal{N}(\mathbf{r}_j))$ of the one-neighborhood $\mathcal{N}(\mathbf{r}_j)$ of \mathbf{r}_j intersect when either \mathbf{r}_i and \mathbf{r}_j share a common edge or there is a ring $\mathbf{r}_k \diamond \mathbf{r}_j$ as the common one-neighbor of \mathbf{r}_i and \mathbf{r}_j .*

Then $\mathcal{M}_\infty = \mathcal{M}_\mathcal{V} \cup \mathcal{M}_\mathcal{R}$.

3. We also consider the monotonicity of the Dirichlet energy and prove its relation with the topology of the discrete surface.

Theorem 5.3.2 ([14]). *Let $\{\mathcal{M}_i\}_i^\infty$ be the sequence of discrete surfaces constructed from a finite discrete surface \mathcal{M}_0 which at least has one n -ring with $n \neq 6$. The Dirichlet energy of \mathcal{M}_i is bounded from above by the constant independent of n . Moreover, it is monotone decreasing after enough steps if there is no n -ring with $n > 6$, conversely, it is monotone increasing after enough steps if there is no n -ring with $n < 6$.*

Remark. In order to distinguish the definition of *face* between our case and the polyhedra case, we use *ring* (defined in Chapter 2) instead of *face* in the present thesis.

The present thesis is organized as follows:

Chapter 2 introduces the basic notions of discrete surfaces. Taking a topological trivalent graph, a discrete surface can be seen as a network realized by a piecewise linear embedded map in \mathbb{E}^3 . The trivalent structure leads to a natural assignment of the normal vectors at each vertex. Section 2.1 gives the basic definitions of geometric quantities, especially normal vectors, fundamental forms, and curvatures, of the discrete surface. Section 2.2 then defines a notion of discrete minimal surfaces which have vanished mean curvature at each vertex and discrete harmonic surfaces which have all the vertices satisfied the balancing condition. For later use in the numerical experiments, Section 2.3 provides a construction of the central frame and defines the height function at each vertex.

Chapter 3 reviews the fundamental theory of subdivision. Section 3.1 introduces the basic definitions and notations of the subdivision algorithm since all these notions are used continuously in the following chapters. Section 3.2 makes a brief overview of the existing subdivision algorithms and their properties. Section 3.3 gives a general process of a subdivision algorithm in a global view and provides the primary problem in subdivision theory. Section 3.4 introduces the locality of the application of one subdivision algorithm and defined the core construction: invariant neighborhood and subdivision matrix. With the preparation in the previous sections, Section 3.5 discusses the convergence of subdivision algorithms and introduces U. Reif's sufficient condition.

Chapter 4 deals with the construction of subdivision algorithms for the discrete surface as a trivalent graph in \mathbb{E}^3 . Section 4.1 introduced the Goldberg-Coxeter construction for trivalent topological graphs which preserve the trivalent structure for each step of the process. Section 4.2 constructs the *invariant neighborhood* and the corresponding subdivision matrix for the discrete surface. Section 4.3 provides a subdivision algorithm for trivalent graph based on the Goldberg-Coxeter construction on the planar graphs.

Chapter 5 constitutes the core part of this work. The convergent of GC-subdivision which constructed in Chapter 4 has been proved from the view of Dirichlet energy in Section 5.1. Section 5.2 discusses the configuration of the limit space of the subdivision sequence, especially in the un-branched case. As a consequence of the previous sections, the monotonicity of the Dirichlet energy is proved in Section 5.3.

Chapter 6 put the subdivision algorithms into practice and demonstrate the numerical experiments for two specific examples: the Mackay crystal and the C_{60} . Both Gaussian curvatures and mean curvatures have been computed and the existence of singularities has been observed. The numerical results show that the subdivision sequences of Mackay crystal converge to the Schwartz P surface. However in the case of C_{60} , a few singularities have been generated by the subdivision process. Some discussions and explanations of these phenomena are given in the end.

Publications: Parts of the results of this thesis have been included in:

1. Chen Tao, “A Construction of Converging Goldberg-Coxeter Subdivisions of a Discrete Surface”, Kobe math J, submitted.
2. Motoko Kotani, Hisashi Naito, and Chen Tao, “Construction of continuum from a discrete surface by its iterated subdivisions”, Communications in Analysis and Geometry, (arXiv:1806.03531), submitted.

Chapter 2

Discrete Surfaces

There are two preliminary descriptions for embedded discrete objects in three-dimensional space, namely, combinatorial and geometrical. The combinatorial descriptions characterize the discrete elements such as vertices, edges and faces, and the combination between them. Each element is defined by a set of elements from the lower dimension, such as faces are defined by edges, edges are defined by vertices. The geometrical descriptions define where to locate these elements in the three-dimensional space. To be more precise, the combinatorial structure is an abstract underlying space with the information of incidental of its elements. When applying some proper geometric method (we often call it as *realization* in our work) on these underlying structure, one can obtain a discrete object in the three-dimensional space. There are two primary reasons that we treat these two characters separately. One of them is that the realization only gives the geometrical positions of each vertex, the positions of other elements such as edges, faces are defined by the corresponding connectivities described by the combinatorial structure of the abstract underlying space. Another one will be introduced in Chapter 3 Subdivision Theory. In fact, when we consider subdivision methods, we usually describe it by the combinatorial description of discrete objects.

Recent works of discrete geometric objects have been intensively done from the view of polyhedral surfaces in \mathbb{E}^3 . These polyhedral surfaces, for example, triangulation of a given geometrical manifold, are usually described as finite copies of triangles or squares with proper combinatorial rules. Thus they are the two-dimensional geometric objects with the parameterized domains, since each triangle or square can be treated as a closed subset of \mathbb{R}^2 . In this chapter, we address a new approach of discrete surfaces which comes from the original work in [13]. The underlying structure is identified with a topological trivalent graph, that is, it consists of the sets of vertices and edges, moreover, the valence at each vertex should be three. The geometrical description is given by a piecewise linear map, which embeds the trivalent structure in \mathbb{E}^3 . Unlike the polyhedral surfaces, a discrete surface under this definition is more like a *network*, not a “surface” in general sense. However, we can identify the tangent plane at each vertex with the plane uniquely determined by its three nearest neighbors. With the assigned tangent plane as well as the normal vector at each vertex, we can define geometric quantities such as the fundamental forms, Gaussian map, and curvatures. Therefore the trivalent graphs in \mathbb{E}^3 can be equipped with geometries which similar to the smooth surfaces. Under these settings, we discuss the discrete minimal and discrete harmonic surfaces. For later use, we also introduce the notion of the

central frame and height function near each vertex. The following definitions are based on those described in [13, 37].

2.1 Trivalent graphs in \mathbb{E}^3 and their curvatures

We firstly start from the combinatorial description. One should notice that each element is described topologically, that is, we only concentrate on the incidental relations.

Let V be a finite set of vertices

$$V = \{v_i | i \in \mathbb{Z}_I = \{0, 1, \dots, I-1\}\}.$$

An edge $e_{ij} = \{v_i, v_j\}$ is a pair of two vertices in V . If two vertices $v_i, v_j \in V$ ($i \neq j$) are connected by one edge, we say $v_i \sim v_j$. Let E be the set of edges that joins two different vertices

$$E \subset \{e_{ij} | e_{ij} = \{v_i, v_j\}, i, j \in \mathbb{Z}_I, i \neq j\}.$$

For any $v \in V$, E_v denotes the set of edges that emerge from v .

Let $X = (V, E)$ be a topological graph with V as the set of vertices and E as the set of edges. We would like to introduce the concept of *ring*. In particular, we call a circuit, which is a closed simple curve without self-intersections, as a *ring* in X . An n -ring r is given by

$$r = \{v_0, \dots, v_{n-1}\}$$

with the ordered n different vertices $v_i \in V$ in the circuit, where $v_i \sim v_{i+1}$ ($i \in \mathbb{Z}_n$) and $v_n = v_0$. Let

$$R = \{r_k | r_k = \{v_{k_0}, \dots, v_{k_{n-1}}\}, k = \{k_0, \dots, k_{n-1}\}, k_i \in \mathbb{Z}_I\}$$

denotes the set of rings. For any $r_k \in R$, we can define the corresponding set of ring edges

$$E(r_k) = \{e_{k_0 k_1}, e_{k_1 k_2}, \dots, e_{k_{n-1} k_0}\}.$$

It is obvious that the size of $E(r_k)$ equals to the length of r_k .

Definition 2.1.1 (Trivalent Graph). Let V be a set of vertices. A trivalent graph $X = (V, E, R)$ is defined by the finite set of vertices V and a finite sets R of rings determined by V and the corresponding set of edges E , which satisfies for any $v \in V$

$$\sharp E_v = 3.$$

For a given a trivalent graph X , we define a *discrete surface* \mathcal{M} in \mathbb{R}^3 by a piecewise linear map

$$\Phi: X \rightarrow \mathbb{E}^3$$

with $\mathcal{M} = \Phi(X)$. Here we mean by “piecewise linear”, the image of each edge e_{ij} , which is determined by its vertices $V(e_{ij}) = \{v_i, v_j\}$, is given by the line segment connecting two vertices, that is

$$\Phi(e_{ij}) = \Phi(V(e_{ij})) = \{\Phi(v_i), \Phi(v_j)\}.$$

Definition 2.1.2 (Discrete Surface). An injective piecewise linear realization $\Phi: X \rightarrow \mathbb{E}^3$ of a trivalent graph X is said to be a discrete surface in \mathbb{E}^3 if

1. for any $v \in V$, all the elements of $\{\Phi(e) | e \in E_v\}$ are linearly independent in \mathbb{E}^3 , where $\Phi(e)$ is determined by the vertices of e , e.g., $\Phi(e) = \Phi(V(e))$.
2. $\Phi(X)$ is locally oriented, that is, the order of the three edges in E_v is assumed to be assigned to each vertex of X .

Given a discrete surface $\Phi: X \rightarrow \mathbb{E}^3$ with $\mathcal{M} = \Phi(X)$. Since Φ is injective, we can define the elements in the image $\mathcal{M} = \Phi(X)$ by the image of the corresponding elements in X . The set of vertices of \mathcal{M} is obtained by the image of V , denoted by

$$\mathcal{V} = \{\mathbf{v} = \Phi(v) | v \in V\},$$

the set of edges of \mathcal{M} is obtained by the image of E , denoted by

$$\mathcal{E} = \{\mathbf{e} = \Phi(e) | \Phi(e) = \Phi(V(e)), e \in E\},$$

and the set of rings of \mathcal{M} is obtained by the image of R , denoted by

$$\mathcal{R} = \{\mathbf{r} = \Phi(r) | \Phi(r) = \Phi(V(r)), r \in R\}.$$

One can see \mathcal{M} can be identified by \mathcal{V} directly since the other elements and the corresponding incidental relations are induced from X immediately after \mathcal{V} be determined.

For any $v \in V$, let v_i be its nearest neighbors, i.e., $v_i \sim v$, and $e_i = \{v, v_i\}$ with $i \in \{1, 2, 3\}$. Then $E_v = \{e_1, e_2, e_3\}$. We call the pair

$$\tau(v) := (v, E_v)$$

as the *basic unit* of v in X . Immediately we have the corresponding element in \mathcal{M} , i.e., $\mathcal{E}_v = \{\mathbf{e}_1, \mathbf{e}_2, \mathbf{e}_3\}$ where $\mathbf{e}_i = \{\mathbf{v}, \mathbf{v}_i\}$ in \mathcal{M} , and the basic unit of \mathbf{v}

$$\tau(\mathbf{v}) = \tau(\Phi(v)) = \Phi(\tau(v)) = (\Phi(v), \Phi(E_v)) = (\mathbf{v}, \mathcal{E}_v).$$

Roughly speaking, \mathcal{M} acts as a one-dimensional “net” in \mathbb{E}^3 with many “holes”. At each knot of the net, we have specific incidental that comes from the basic unit so that we can equip the abstract knot with geometry structures. On the other hand, the “holes” can be identified with rings in \mathcal{M} which is a circuit of vertices, or in fact, a cyclic combination of copies of the basic unit. How to fill these “holes” by the basic unit is one of the fundamental problems in the theory of discrete surfaces. Before we state the core problem, we take a brief review of the geometry structure on this “net”.

Definition 2.1.3 (Tangent Plane). Let $\Phi: X \rightarrow \mathbb{E}^3$ be a discrete surface with $\mathcal{M} = \Phi(X)$. For any $\mathbf{v} \in \mathcal{M}$, the *tangent plane* $T_{\mathbf{v}}\mathcal{M}$ and the corresponding *unit normal vector* $n(\mathbf{v})$ can be defined by the basic unit $\tau(\mathbf{v}) = (\mathbf{v}, \mathcal{E}_v)$. That is,

$T_{\mathbf{v}}\mathcal{M}$ is identified with the plane uniquely determined by \mathbf{v} ’s nearest neighbors $\{\mathbf{v}_1, \mathbf{v}_2, \mathbf{v}_3\}$ and the *unit normal vector* $n(\mathbf{v})$ at \mathbf{v} is given by

$$(2.1.1) \quad n(\mathbf{v}) = \frac{\mathbf{e}_1 \times \mathbf{e}_2 + \mathbf{e}_2 \times \mathbf{e}_3 + \mathbf{e}_3 \times \mathbf{e}_1}{|\mathbf{e}_1 \times \mathbf{e}_2 + \mathbf{e}_2 \times \mathbf{e}_3 + \mathbf{e}_3 \times \mathbf{e}_1|},$$

where $\mathbf{e}_i \in \mathcal{E}_v, \mathbf{e}_i = \{\mathbf{v}, \mathbf{v}_i\}$.

Remark 2.1.4. Let $\tau = \tau(\mathbf{v})$ be a basic unit. $\tau_i = \tau(\mathbf{v}_i)$ be the unit of \mathbf{v}_i , where \mathbf{v}_i is the nearest neighbor of \mathbf{v} . Then we can define the following geometry quantities at each vertex \mathbf{v} by τ and τ_i .

1. The *directional derivative* of Φ at \mathbf{v} along e_i is given as the orthogonal projection of e_i to the tangent plane $T_{\mathbf{v}}\mathcal{M}$, i.e.,

$$(2.1.2) \quad \nabla_{e_i}\Phi = \text{Proj}[\Phi(e_i)] = \text{Proj}[e_i] = e_i - \langle e_i, n(\mathbf{v}) \rangle e_i.$$

2. The *directional derivative* of the unit normal vector at \mathbf{v} along e_i is given by

$$(2.1.3) \quad \nabla_{e_i}n(\mathbf{v}) = \text{Proj}[n(\mathbf{v}_i) - n(\mathbf{v})].$$

3. The *first* and *second fundamental forms* of $\mathbf{v} \in \mathcal{M}$ are given by, respectively

$$(2.1.4) \quad \begin{aligned} \text{I}(\mathbf{v}) &= \begin{pmatrix} \langle e_2 - e_1, e_2 - e_1 \rangle, & \langle e_2 - e_1, e_3 - e_1 \rangle \\ \langle e_3 - e_1, e_2 - e_1 \rangle, & \langle e_3 - e_1, e_3 - e_1 \rangle \end{pmatrix}, \\ \text{II}(\mathbf{v}) &= \begin{pmatrix} -\langle e_2 - e_1, n_2 - n_1 \rangle, & -\langle e_2 - e_1, n_3 - n_1 \rangle \\ -\langle e_3 - e_1, n_2 - n_1 \rangle, & -\langle e_3 - e_1, n_3 - n_1 \rangle \end{pmatrix}. \end{aligned}$$

where $n_i = n(\mathbf{v}_i)$, $i \in \{1, 2, 3\}$. Notice that $\text{II}(\mathbf{v})$ is not necessarily symmetric.

Definition 2.1.5 (Curvatures). Let $\Phi: X \rightarrow \mathbb{E}^3$ be a discrete surface with $\mathcal{M} = \Phi(X)$. Then for each vertex $\mathbf{v} \in \mathcal{M}$, the *Gauss curvature* $K(\mathbf{v})$ and the *mean curvature* $H(\mathbf{v})$ are represented as follows, respectively

$$(2.1.5) \quad \begin{aligned} K(\mathbf{v}) &= \det[\text{I}(\mathbf{v})^{-1} \text{II}(\mathbf{v})], \\ H(\mathbf{v}) &= \frac{1}{2} \text{tr}[\text{I}(\mathbf{v})^{-1} \text{II}(\mathbf{v})]. \end{aligned}$$

Example 2.1.6. (1) Regular hexahedron and (2) regular truncated icosahedron (fullerene C_{60}) are both trivalent graph in \mathbb{E}^3 with constant curvatures.

Proof. Since both of them are regular and located on the sphere, we can consider a basic unit τ on sphere with $\mathbf{v} = r n(\mathbf{v})$ where r is the radius. It is easy to check $e_i - e_1 = r(n_i - n_1)$ thus we have

$$\text{I}(\mathbf{v}) = -r \text{II}(\mathbf{v}).$$

That is

$$K(\mathbf{v}) = \frac{1}{r^2}, \quad H(\mathbf{v}) = -\frac{1}{r}.$$

□

2.2 Discrete harmonic and discrete minimal surfaces

In smooth surface theory, conformal minimal immersions of Riemann surfaces in \mathbb{R}^3 are harmonic maps. How are they related under the discrete version? Since we have already defined the mean curvature at each vertex, it is very natural to have the following definition of discrete minimal surface.

Definition 2.2.1 (Discrete Minimal Surface). A discrete surface $\Phi: X \rightarrow \mathbb{E}^3$ is called a discrete minimal surface if its mean curvature vanishes at each vertex.

Harmonic map is the critical point of Dirichlet functional. In our settings, Dirichlet energy is defined on the discrete elements. Let $\Phi: X \rightarrow \mathbb{E}^3$ with $\mathcal{M} = \Phi(X)$ be a discrete surface. By the definition we know X is finite, thus we define the *Dirichlet energy* E_D of $\Phi(X)$ by the sum of square norm of all edges, i.e.,

$$(2.2.1) \quad E_D(\Phi(X)) = \sum_{e \in E} |\Phi(e)|^2.$$

Furthermore, the realization of an arbitrary graph X that minimizes the Dirichlet energy is called as a *harmonic realization* [16] or an *equilibrium placement* [5].

In fact, the harmonic realization introduces a distinct local geometric feature. Let $\tau = (v, E_v)$ be the basic unit of X , from an elementary result in classical geometry, the Dirichlet energy

$$(2.2.2) \quad E_D(\Phi(\tau)) = |\Phi(e_1)|^2 + |\Phi(e_2)|^2 + |\Phi(e_3)|^2$$

reaches its minimum if and only if $\Phi(v)$ is located at the barycenter of its nearest neighbors. By this fact, we give the following definition

Definition 2.2.2 (Harmonic Discrete Surface ([13, Definition 3.15])). A discrete surface $\Phi: X \rightarrow \mathbb{E}^3$ is harmonic when it satisfies

$$(2.2.3) \quad \Phi(e_{v,1}) + \Phi(e_{v,2}) + \Phi(e_{v,3}) = 0,$$

for any $v \in V$, and $E_v = \{e_{v,1}, e_{v,2}, e_{v,3}\}$.

The equation (2.2.3) is called as the *balancing condition*. The representation of curvatures of harmonic discrete surface are computed as following

Proposition 2.2.3 ([13, Proposition 3.16]). Let $\Phi: X \rightarrow \mathbb{E}^3$ be a discrete harmonic surface, for $v \in V$ and $E_v = \{e_1, e_2, e_3\}$, the Gauss curvature $K(\mathbf{v})$ and the mean curvature $H(\mathbf{v})$ are respectively given by

$$(2.2.4) \quad \begin{aligned} K(\mathbf{v}) &= -\frac{3}{2A(\mathbf{v})^2} \sum_{i,j,k} \langle \mathbf{e}_i, \mathbf{n}_j \rangle \langle \mathbf{e}_j, \mathbf{n}_i \rangle, \\ H(\mathbf{v}) &= \frac{3}{2A(\mathbf{v})^2} \sum_{i,j,k} \langle \mathbf{e}_i, \mathbf{e}_j \rangle (\langle \mathbf{e}_i, \mathbf{n}_j \rangle + \langle \mathbf{e}_j, \mathbf{n}_i \rangle), \end{aligned}$$

where $A(\mathbf{v}) = \det[\mathbf{I}(\mathbf{v})]$, (i, j, k) is the alternate of $(1, 2, 3)$.

Proposition 2.2.3 indicates that a discrete harmonic surface may not be discrete minimal. The following theorem provides a sufficient condition for a discrete harmonic surface which has vanished mean curvature at each vertex.

Theorem 2.2.4 ([13, Theorem 3.17]). A discrete harmonic surface $\Phi: X \rightarrow \mathbb{E}^3$ is minimal if for any $v \in V$ and $E_v = \{e_1, e_2, e_3\}$

$$(2.2.5) \quad \langle \Phi(e_1), \Phi(e_2) \rangle + \langle \Phi(e_2), \Phi(e_3) \rangle + \langle \Phi(e_3), \Phi(e_1) \rangle = 0.$$

In particular, the equation above is equivalent to

$$(2.2.6) \quad |\Phi(e_1)| = |\Phi(e_2)| = |\Phi(e_3)|.$$

2.3 Central frame and height function

As we mentioned before, unlike polyhedral meshes, an embedded trivalent graph is a discrete object in \mathbb{E}^3 without any information about the underlying surface. Given a polyhedral mesh, for example, triangulation. It can be viewed as combined copies of the triangle with geometric information. Each triangle is a closed subset of \mathbb{R}^2 and equipped with the smooth coordinate inside. However, in our setting, the discrete surface can be represented as finite copies of the basic unit with combinatorial rules. Although the trivalent feature of the basic unit provide a “natural” way for us to define the geometric structures, its underlying space can hardly have any proper coordinate. Fortunately, in the classical surface theory, by assuming some requirements, a surface can be locally expressed in *Euler form*. To be more precisely, it can be viewed as the graph of a scalar-valued function in a local coordinate system, that is, the parameters are associated with the tangent plane moreover, the function values are measured in the normal direction. We call this function the height function. The smoothness nearby is related to the differentiability properties of this height function.

We address this issue in the following way. Let $\Phi: X \rightarrow \mathbb{E}^3$ with $\mathcal{M} = \Phi(X)$ be a discrete surface. For a fix vertex $\mathbf{v}_0 \in \mathcal{M}$, assume \mathbf{v}_0 is located at the origin. Take the unit normal vector $\mathbf{n}_0 = n(\mathbf{v}_0)$ as the z -direction. Then the xy -plane becomes the tangent plane of \mathbf{v}_0 .

Let $T_0 = (t_1^{(0)}, t_2^{(0)})$ be a pair of two linear independent vectors on $T_{\mathbf{v}_0}\mathcal{M}$. Define

$$(2.3.1) \quad F_0 := [T_0, \mathbf{n}_0]$$

as the *central frame* at \mathbf{v}_0 , which is a 3×3 -matrix. Assuming there exists a neighborhood $\delta(\mathbf{v}_0)$ of \mathbf{v}_0 such that the orthogonal projection of these vertices to the tangent plane at \mathbf{v}_0 is injective, in fact, at least the nearest neighbors of \mathbf{v}_0 satisfied this requirement. Then under the central frame, any $\mathbf{v} \in \delta(\mathbf{v}_0)$ has

the *tangential component*

$$(2.3.2) \quad \xi_0 = (\mathbf{v} - \mathbf{v}_0) \cdot T_0 \in \mathbb{R}^2$$

the *normal component*

$$(2.3.3) \quad \zeta_0 = (\mathbf{v} - \mathbf{v}_0) \cdot \mathbf{n}_0 \in \mathbb{R}.$$

the local *height function*

$$(2.3.4) \quad h(\xi_0) = \zeta_0$$

Then we have the following unique representation of \mathbf{v}

$$(2.3.5) \quad \mathbf{v} = \mathbf{v}_0 + \xi_0 T_0 + h(\xi_0) \mathbf{n}_0,$$

and the local *Euler form*

$$(2.3.6) \quad (\mathbf{v} - \mathbf{v}_0) \cdot F_0 = [\xi_0, h(\xi_0)].$$

Remark 2.3.1. Let \mathbf{v}_i be a nearest neighbor of \mathbf{v} , then the absolute value of the height function on \mathbf{v}_i measures the distance between \mathbf{v} and the bottom $\triangle(\mathbf{v}_1, \mathbf{v}_2, \mathbf{v}_3)$. In particular, when $\Phi: X \rightarrow \mathbb{E}^3$ is discrete harmonic, this height vanishes.

Chapter 3

The Fundamental Theory of Subdivision

Subdivision algorithms are developed from two opposite motivations. Usually, one of the motivations is to approximate a given surface over a *control net*, for example, triangulation of a geometric surface. To do so, one may try to refine the control net by some “well defined” rules which is called as the subdivision. By applying subdivision repeated, more and more elements such as vertices and corresponding combinatorial structures are inserted into the control net so that they converge to the original surface under some proper conditions. From the other side, one can define the subdivision algorithms by applying a linear map on a given space of control net without knowing any information about the underlying surface. The subdivision algorithms can be processed iteratively so that one can obtain a sequence of control nets. If this sequence converged in some certain sense, one might use this procedure to find the underlying surface, or in general, to generate a surface. Therefore, by considering both of the views, one can use subdivision algorithm to deal with the problem of filling a “hole” on a given surface, or equivalently, finding an underlying surface from a given mesh.

In this section, we present a short introduction of subdivision theory, such as original ideas, general subdivision process and analysis near the singularities. Some fundamental properties are also discussed so that one can make a better understanding of the subdivision algorithms as well as the structure of the combinatorial meshes.

3.1 Control net and refinement

A *Control net* in subdivision theory is a discrete object where the subdivision algorithms act. Polyhedral meshes, triangulations and the discrete surfaces we introduced in Chapter 2 are all examples of control nets.

As we mentioned, a discrete object is usually described by the combination of discrete elements and geometry information. Using arguments similar to those in Chapter 2 (*normal* type for the elements in the topological graph and ***bold*** type for the corresponding elements in \mathbb{E}^3), let K be combinatorial mesh, which consists of vertices with incidental relations. An injective map $\Phi: K \rightarrow \mathbb{E}^3$ and $\mathcal{C} = \Phi(K)$ defines a control net in \mathbb{E}^3 with the combinatorial structure described by K .

We put an extra line here, in this chapter, we use combinatorial meshes and control nets instead of the topological graphs and the corresponding realizations that we defined in Chapter 2, respectively. The formers are often used in the general subdivision theory.

Definition 3.1.1 (Valence). Let $\Phi: K \rightarrow \mathbb{E}^3$ with $\mathcal{C} = \Phi(K)$ be a control net. The valence of a vertex $v \in K$ (corresponding with $\mathbf{v} \in \mathcal{C}$) is given by the number of edges emerged from it.

The vertices of a given control net can be classified into two types in terms of valence: the *ordinary vertex* and the *extraordinary vertex*. Here the valence of the vertices should be considered after several steps of refinement. Therefore, this classification is also related to subdivision algorithms. That is, after several steps of refinement, the vertices with the most appeared valence are called to be the ordinary vertices. The rest are called to be the extraordinary vertices. Always, the regular tiling of a plane by individual polygons gives a hint of this classification. For example, the ordinary vertices of the triangular mesh are those vertices with valence six, and the ordinary vertices of the square mesh are those vertices with valence four (see Figure 3.1).

Remark 3.1.2. A control net with all vertices that have the same valence is called as *regular*, otherwise is called as *irregular*. In particular, a control net with all vertices have the same valence except for one with valence ν is called as ν -regular.

For each vertex of a given control net, we consider the combinatorial structures nearby as the following

Definition 3.1.3 (One-/n-neighborhood). Let $\Phi: K \rightarrow \mathbb{E}^3$ with $\mathcal{C} = \Phi(K)$ be a control net. For a given vertex $v \in K$ (corresponding with $\mathbf{v} \in \mathcal{C}$), the set of all faces which have v (\mathbf{v}) as the common vertex is called as the one-neighborhood of v (\mathbf{v}). Inductively, the union of the one-neighborhoods of all vertices in the $(n-1)$ -neighborhoods of v (\mathbf{v}) is called as the n -neighborhood.

In particular, the neighborhood of the ordinary vertex is called as the *regular region* and the neighborhood of the extraordinary vertex is called as the *irregular region* (see Figure 3.1).

Given a control net \mathcal{C} with K as its combinatorial mesh. Let \mathcal{V} be the set of vertices of \mathcal{C} . The refinement of \mathcal{C} is construct by two basic steps:

1. Insert new vertices to \mathcal{V} based on the combinatorial description.
2. Connecting appropriate vertices and generating a new control net \mathcal{C}' .

By considering the combinatorial structure of the new control net \mathcal{C}' , the refinement can be characterized into two types: *interpolate type* where the vertices from \mathcal{V} also take part in the incidental relation of \mathcal{C} and *approximate type* where the inserted vertices are prescribed in a similar way of \mathcal{C} , however, do not connect with its vertices. The interpolate type remains the geometry information of the initial control net. One of the examples is given as the split operation over the square mesh. For a square mesh, adding one vertex for each edge and one vertex for each face. Keeping the split edges and connecting the face vertex with the inserted edge vertices such that each square face splits into four. The approximate type may generate a surface with C^k -continuous ($k > 2$). Corner cutting is one such type of refinement. By cut off the vertices and the edges, the resulting edges and the new vertices are meet at the vertex cutoffs.

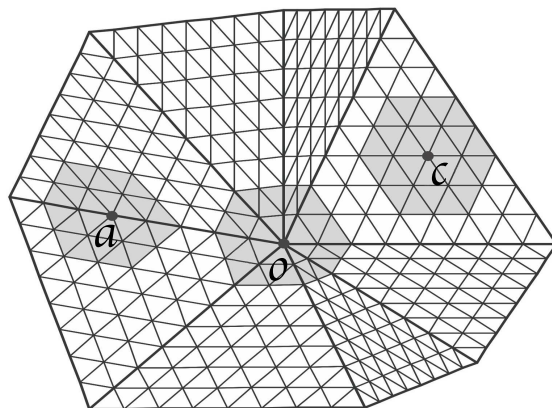


Figure 3.1: Both a and c are the ordinary vertices with their 2-neighborhood as the regular region. o is the extraordinary vertex with its 2-neighborhood as the irregular region.

3.2 Subdivision zoo

For a given polyhedral mesh as control net, a subdivision algorithm produces a sequence of the control nets with increasing finer geometrical structure. E. Catmull and J. Clark [4] and D. Doo and M. Sabin [7] introduced the first geometric subdivision algorithm. They assumed that a given control net consists of two types of regions, one is called as the *regular region*, where the standard continuity can be introduced and the other one is called as the *irregular region*, where the continuity is not easy to achieve. Thus the resulting surface also consists of continue part which corresponding to the regular regions and “holes” which corresponding to the irregular regions. Moreover, the subdivision algorithm enlarges the regular regions and shrinks the irregular regions without changing the number and the type so that the “holes” can be filled gradually. In the space of control net, this means when we insert new vertices, most of them are located to match the conditions of the regular regions, however, those vertices that contribute to generate shrinking irregular region should be chosen rather than arbitrarily. Often, they are computed by some linear combination of the vertices from the old control net near the irregular region, which are also called as *invariant neighborhood* sometimes. The associated matrix of this combination is called as the *subdivision matrix*. The smoothness of the limit surface is deeply related to the choice of this matrix when the subdivision algorithm is applied iteratively.

After the initial idea of Catmull-Clark subdivision and Doo-Sabin subdivision, C. Loop [18] developed the Loop subdivision as well as N. Dyn [8] developed the Butterfly subdivision for triangular meshes. They followed the original idea and extended the algorithm from quad mesh to triangles. Various of subdivision algorithms have been developed for specific requirements and applications to different fields such as computer graphics, industrial design, and engineering. J. Stam and C. Loop [35] combined both the Catmull-Clark subdivision and the Loop subdivision, and invented the Quad/triangle algorithm. They applied both algorithms separately on the quad and triangle part from a mixed quad and triangle mesh and introduced new subdivision rules for the connecting parts. Although this method loses some continuity on the connecting elements, it has improved the Catmull-Clark subdivision in handling with the undesirable triangular parts from quad meshes

and made this method more applicable under several conditions. To construct surfaces with a particular property, G. Morin [21] uses cubic polynomials to generate circles and hyperbolic functions in the subdivision and designed the Circle preserving subdivision. In this subdivision algorithm, a tension parameter is introduced so that one can obtain an almost everywhere C^2 -continuous surface except for a finite number of vertices which is C^1 -continuous. Other motivations like taking great control of the size of refined mesh has been considered as well. The simplest subdivision by U. Reif and J. Peters [32], the 4–8-subdivision by L. Velho and D. Zorin [38], and the $\sqrt{3}$ -subdivision by L. Kobbelt [12] are addressed as the subdivision algorithms which has a smaller number of newly inserted vertices. Furthermore, Free-form splines by H. Prautzsch [29] and TURBS by U. Reif [31] are notable for their high smoothness. Both of these algorithms can generate a surface with an arbitrary degree of smoothness. The basic techniques are based on the functions of bi-degree $(2k + 2)$ and can generate C^k -continuous surfaces.

We list typical subdivision algorithms with a short explanation about the properties in Table 3.2, which is called as the Subdivision Zoo. One can check almost all the subdivision algorithms have been constructed to generate quad or triangular meshes. Some of the algorithms construct a new control net interpolating with the initial one. Others focus on the smoothness requirement and design the approximate approaches. In fact, C^1 -(normal) continuous and C^2 -(curvature) continuous can be satisfied. With some specific method, one can even construct C^k -continuous surfaces. However, all of these algorithms have singularities in the limit surface. Here the singularity means the point where the well-behaved differentiability fails. For example, Catmull-Clark subdivision generates an almost C^2 -continuous surface with some individual vertices (in fact, the extraordinary vertex of the control net) have C^1 -continuous.

Subdivision Algorithm	Net	Type	Degree	Class
Catmull-Clark [E. Catmull and J. Clark [4]]	□	approx	bicubic	C^2
Doo-Sabin [D. Doo and M. Sabin [7]]	□	approx	biquadratic	C^2
Loop [C. Loop [18]]	△	approx	quartic	C^2
Butterfly [N. Dyn et al [8]]	△	interpol		C^1
Kobbelt [L. Kobbelt [11]]	□	interpol		C^1
Simplest [U. Reif and J. Peters [32]]	□	approx	quadratic	C^1
TURBS [U. Rief [31]]	□	approx	bi- $2k + 2$	C^k
$\sqrt{3}$ -Subdivision [L. Kobbelt [12]]	△	approx		C^2
4-8 Subdivision [L. Velho and D. Zorin [38]]	△	approx	sixtic	C^4
Circle preserving [G. Morin et al [21]]	□	approx	cubic	C^2
Ternary triangle [C. Loop [19]]	△	approx	quartic	C^4
Quad/triangle [J. Stam and C. Loop [35]]	△, □	approx	bicubic, quartic	C^2
4-3 [J. Peters and L. Shiue [23]]	△, □	approx	quartic	C^2
$\sqrt{2}$ -Subdivision [Li et al [17]]	□	interpol	sixtic	C^4

Table 3.1: *Subdivision Zoo*. A brief introduction of typically subdivision algorithms and their basic properties.

3.3 Subdivision process

Subdivision process is the way to produce sequences of control nets by applying the subdivision algorithms iterated. As we mentioned before, the basic idea of the subdivision is to define a smooth object as the limit of a sequence of successive refinement. Thus the sequence of control nets should be finer when the subdivision algorithms applied adjectively on the initial control net. This means the newly generated control net will have a greater number of discrete elements, such as vertices, edges, and faces. We often take subdivision process as operations act on the control net.

To be more precise, let $\Phi: K \rightarrow \mathbb{E}^3$ with $\mathcal{C} = \Phi(K)$ be a given control net, each step of the subdivision process is described by a set of similar operations. Furthermore, individual step of the subdivision process is described by two operations. One is the refinement operation on the combinatorial mesh K , which produces new vertices and combinatorial descriptions to generate K' . Another one is the smoothing operation in which we assign the geometrical description to the new K' , that is, $\Phi': K' \rightarrow \mathbb{E}^3$ with $\mathcal{C}' = \Phi'(K')$ as the new generated control net from \mathcal{C} .

Although the subdivision algorithm changes the global view of control nets, the process is local. That is, newly added vertices are derived from the vertices in a fairly small neighborhood of each vertex from the previous control net. This derivation can be described by a linear combination, which can also be treated as a weighted sum of the vertices in the previous control net. A *subdivision mask* is a weighted graph. The weight of the vertices in the previous control net are used to compute a particular new vertex after one step of the subdivision (see Figure 3.2).

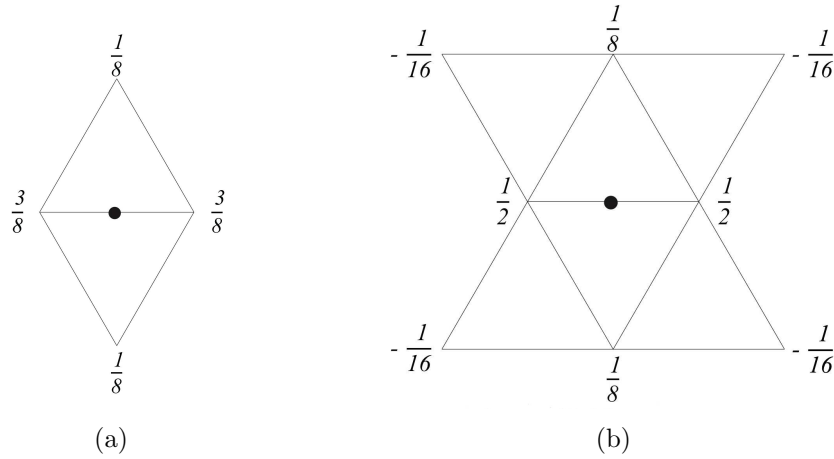


Figure 3.2: (a) A subdivision mask from the Loop subdivision. (b) A subdivision mask from the Butterfly subdivision.

Usually, we let the sum of the weights from one given mask equals to one. Furthermore, by the idea of E. Catmull and J. Clark [4], the generated vertices should be ordinary while the number and the type of the extraordinary vertices are constant during the iterative subdivision process. From the view of configuration, this requirement makes sure that the extraordinary vertices are isolated from each other after several steps of the subdivision. By the locality of subdivision masks, the corresponding process can be split into a combination of local refinements.

Now we start with a general case of subdivision process. Let \mathcal{C}_0 be a given control net with K as its combinatorial mesh

$$(3.3.1) \quad \Phi: K \rightarrow \mathbb{E}^3 \text{ with } \mathcal{C} = \Phi(K).$$

A subdivision is processed by iteration of the subdivision algorithm over the initial control net to generate a sequence of control nets as a chain

$$(3.3.2) \quad \mathcal{C}_0 \rightarrow \mathcal{C}_1 \rightarrow \cdots \rightarrow \mathcal{C}_i \rightarrow \cdots,$$

where \mathcal{C}_i refers to the control net of each step and “ \rightarrow ” defined the process direction. The \mathcal{C}_i is obtained by \mathcal{C}_{i-1} and is rooted in \mathcal{C}_0 .

For any control net \mathcal{C}_i , let $\mathcal{V}_i = \{\mathbf{v}_k^i | k \in \mathbb{Z}_{I_i}\}$ be the set of the vertices. By the discussion in Chapter 2 we can identify \mathcal{C}_i with \mathcal{V}_i . In particular, \mathcal{C}_i can be described by a *control net matrix*

$$(3.3.3) \quad C_i := (\mathbf{v}_0^i, \mathbf{v}_1^i, \dots, \mathbf{v}_{I_i-1}^i)^t.$$

where C_i has the size of $(I_i \times 3)$ and each row refers to a vertex in three dimensional space. The vertices of \mathcal{C}_i is generated from the vertices of the previous control net. Furthermore, this relation is linear. Therefore the subdivision process can be described by the following map

$$(3.3.4) \quad \mathcal{S}: \mathcal{C}_i \rightarrow \mathcal{C}_{i+1}$$

in the view of control net matrix

$$(3.3.5) \quad C_{i+1} = SC_i,$$

where S is an adaptive matrix called the *global subdivision matrix*. The map \mathcal{S} constructs the combinatorial structure of K_{i+1} from K_i and describes the geometrical position of each vertex in K_{i+1} . Formally, we use the same “ S ” to represent the corresponding matrix. In fact, as the subdivision process goes on, the size of S keeps growing since the number of vertices increases after each step of subdivision. For each control net \mathcal{C}_i , one can trace back to the initial one by

$$(3.3.6) \quad C_i = SC_{i-1} = S^2C_{i-2} = \cdots = S^iC_0.$$

where S^i refers to the formal product of S with increasing size. The restriction of S on a proper neighborhood of a vertex is nothing but the subdivision mask. That is, S can be represented by the weights that we use to generate new vertices from the previous control net. By applying S for infinite many times, we can get the following sequence

$$(3.3.7) \quad \mathcal{C}_0 \rightarrow \mathcal{C}_1 \rightarrow \cdots \rightarrow \mathcal{C}_i \rightarrow S^\infty \mathcal{C}_0$$

If the subdivision algorithm converges, then we have

$$(3.3.8) \quad S^\infty \mathcal{C}_0 = \lim_{i \rightarrow \infty} S^i C_0$$

as the *limit surface*. Here we use the expressions of “convergence” and “limit” without specifying definitions.

3.4 Invariant neighborhood and subdivision matrix

Since the size of the global subdivision matrix keeps increasing after each step of the process, the investigation of subdivisions from the global view is not easy to achieve. Because of the locality we discussed before, however, the control net \mathcal{C}_{i+1} can be generated by application of some subdivision masks piece by piece on a partition of \mathcal{C}_i . The global issue can be split into a combination of local refinements with specific properties. In another word, the subdivision algorithm generates a shrinking irregular/regular region by producing a sequence of shrink n -neighborhoods of a given extraordinary/ordinary vertex. This shrinking process is also called as “prolongation” of the regular regions since the irregular regions can be treat as “gaps” after several steps of the subdivision. The matrix constructed by the combination of the subdivision masks of the vertices in this n -neighborhood is called as the *subdivision matrix* and the associated n -neighborhood is called as the *invariant neighborhood*. Additionally, this subdivision matrix should preserve the combinatorial structure of the invariant neighborhood, and remains unchanged for each subdivision step.

Definition 3.4.1 (Subdivision matrix). Let \mathcal{C}_0^N be an n -neighborhood of a specific vertex in \mathcal{C}_0 with the combinatorial mesh N . Let \mathcal{S}_N be the local subdivision map that determines the subdivision near the vertex and preserves the combinatorial structure of N . That is

$$(3.4.1) \quad \begin{aligned} \mathcal{S}_N: \mathcal{C}_i^N &\rightarrow \mathcal{C}_{i+1}^N \\ \mathcal{C}_{i+1}^N &= S_N \mathcal{C}_i^N \end{aligned}$$

The associated matrix S_N is called as the subdivision matrix and the control net matrix \mathcal{C}_i^N is called as the invariant neighborhood.

In the Loop subdivision [18], the invariant neighborhood is the 2-neighborhood of a extraordinary vertex as shown in Figure 3.3.

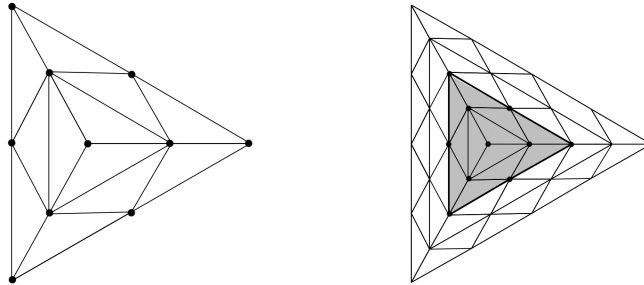


Figure 3.3: The invariant neighborhood of the Loop subdivision.

Suppose \mathcal{C}_0^N has k vertices. Then the control net matrix \mathcal{C}_0^N has the size of $k \times 3$. The corresponding subdivision matrix S_N act on \mathcal{C}_0^N by matrix product as following

$$(3.4.2) \quad S_N \begin{pmatrix} \mathbf{v}_{N_0}^0 \\ \mathbf{v}_{N_1}^0 \\ \mathbf{v}_{N_1}^0 \\ \dots \\ \mathbf{v}_{N_{k-1}}^0 \end{pmatrix} = \begin{pmatrix} \mathbf{v}_{N_0}^1 \\ \mathbf{v}_{N_1}^1 \\ \mathbf{v}_{N_1}^1 \\ \dots \\ \mathbf{v}_{N_{k-1}}^1 \end{pmatrix}.$$

Moreover, the size of S_N is $(k \times k)$ determined by C_0^N and each row of S_N is given by the subdivision mask of the corresponding vertex.

In fact, the subdivision matrix can be viewed as the restriction of the global subdivision matrix on the invariant neighborhood, that is,

$$(3.4.3) \quad S_N = S|_N.$$

Therefore, the investigation on the growing global subdivision matrix can be considered separately on each invariant neighborhood with the associated subdivision matrix. Subdivision matrix plays an essential role in subdivision algorithm rather than related control nets from adjacent subdivision steps. The analysis of the convergence and smoothness properties of the subdivision process, especially at the extraordinary vertices, is based on the eigenstructure of the subdivision matrix.

3.5 Convergence of subdivisions

In this section, we introduce the *Reif's sufficient condition* discussed by U. Reif in [30] for the convergence of the subdivision algorithms.

Let C_0^N be an invariant neighborhood of a given control net C_0 and S_N be the associated local subdivision map. We have the following chain of generated invariant neighborhoods

$$(3.5.1) \quad C_0^N \rightarrow C_1^N \rightarrow \cdots \rightarrow C_i^N \rightarrow$$

with

$$(3.5.2) \quad C_i^N = S_N C_{i-1}^N = S_N^2 C_{i-2}^N = \cdots = S_N^i C_0^N,$$

where S_N is the subdivision matrix with a fixed size which determined by the vertex matrix C_0^N . Moreover, $S_N^i = S_N S_N^{i-1} = S_N S_N \cdots S_N$ is the matrix product. Iterative application of the subdivision matrix generates a sequence of invariant neighborhoods. In particular, if the generated invariant neighborhoods shrinking into one vertex, the local subdivision is said to be *convergent*. That is

Definition 3.5.1. Let C_0^N be a given invariant neighborhood. The associated subdivision map S_N is said to be convergent if there exist a unique vertex \mathbf{v} with

$$(3.5.3) \quad \lim_{i \rightarrow \infty} \mathbf{v}_N^i = \mathbf{v}$$

for any sequence of vertices $\mathbf{v}_N^i \in C_i^N$ where $C_i^N = S_N^i C_0^N$.

Equivalently, this also defined the convergence of subdivision matrix in the corresponding matrix form.

Remark 3.5.2. Let

$$(3.5.4) \quad \mathcal{C} = \bigcup_{i \in \mathbb{N}} C_i^N = \bigcup_{i \in \mathbb{N}} S_N^i C_0^N.$$

The convergence implies the closure

$$(3.5.5) \quad \bar{\mathcal{C}} = \mathcal{C} \cup \mathbf{v}$$

is a surface without gap.

Definition 3.5.3. The surface $\bar{\mathcal{C}}$ is said to be tangent plane continuous, if the subdivision map (or the associated subdivision matrix) converges and if there exist a unique limit $n(\mathbf{v})$ such that for any sequence of normal vectors

$$(3.5.6) \quad \lim_{i \rightarrow \infty} n(\mathbf{v}_N^i) = n(\mathbf{v}),$$

where $\mathbf{v}_N^i \in \mathcal{C}_i^N$.

Remark 3.5.4.

1. $n(\mathbf{v})$ is a formal normal vector as the limit of the converged sequence since the normal vector at $\mathbf{v} \in \bar{\mathcal{C}}$ may not even exist.
2. Being tangent continuous dose not mean C^1 -continuous unless the projection of the vertices to the limit tangent plane is injective, which means the local *single sheeted*.

Furthermore, the subdivision algorithm can be treated as a combination of local subdivision maps over the corresponding invariant neighborhoods. The convergence of a subdivision algorithm therefore can be represented by the convergence of the iterated local subdivision maps as well as the associated subdivision matrices.

When no ambiguity is possible, we identity the invariant neighborhood \mathcal{C}_0^N and the associated local subdivision map \mathcal{S}_N with the corresponding vertices matrix C_0^N and the subdivision matrix S_N , respectively.

Now we start to introduce the Reif's sufficient condition for the convergence of a given subdivision algorithm. It is equivalent to consider the convergence of the subdivision matrix since the global subdivision map is clipping into pieces of local subdivision maps on "well-prepared" invariant neighborhoods.

Let \mathcal{C}_0^N be the invariant neighborhood with S as the associated subdivision matrix. Since each row of S sums up to 1, $\lambda_0 = 1$ is always an eigenvalue of S and $\varphi_0 = (1, 1, \dots, 1)^t$ is the corresponding eigenvector. Let λ_i be the eigenvalues of S and φ_i be the corresponding eigenvector, where $i \in \mathbb{Z}_K$.

Theorem 3.5.5 ([30]). *A subdivision matrix S converged if $1 = \lambda_0 > |\lambda_1| \geq \dots \geq |\lambda_{K-1}|$.*

Proof. Let \mathcal{C}_0^N be the corresponding invariant neighborhood. C_0^N can be expressed by the eigenvectors of S as

$$(3.5.7) \quad C_0^N = \sum_{i=0}^{K-1} \varphi_i a_i.$$

Since C_0^N sized of $(K \times 3)$, φ_i sized with $(K \times 1)$, then $a_i \in \mathbb{R}^3, i \in \mathbb{Z}_K$.

Similarly, the subdivision sequence can be expressed by

$$(3.5.8) \quad C_m^N = S_N^m C_0^N = \sum_{i=0}^{K-1} \lambda_i^m \varphi_i a_i = (a_0, a_0, \dots, a_0)^t + o(1).$$

Which means for any $\mathbf{v}_N^m \in C_m^N$, we have

$$(3.5.9) \quad \mathbf{v}_N^m = a_0 + o(1).$$

Let $\mathbf{v} = a_0$, therefore we have

$$(3.5.10) \quad \lim_{m \rightarrow \infty} \mathbf{v}_N^m = \mathbf{v}.$$

□

Suppose a_0 is at the origin. Additionally and without loss of generality, we assume $\lambda_1 = \lambda_2 = \lambda > 0$. Then we have

$$(3.5.11) \quad C_m^N = \lambda^m (\varphi_1 a_1 + \varphi_2 a_2 + o(\frac{\lambda_3}{\lambda})^m).$$

Equation 3.5.11 shows that, up to a scaling factor λ^m , any $\mathbf{v}_{N_j}^m \in C_m^N$ with sufficient large m , it can be express by the linear combination of a_1 and a_2 , up to an infinite small term

$$(3.5.12) \quad \frac{\mathbf{v}_{N_j}^m}{\lambda^m} = (\varphi_1)_j a_1 + (\varphi_2)_j a_2 + (o(\frac{\lambda_3}{\lambda})^m),$$

where $(\cdot)_j$ means the element from j -th row.

This indicates that a_1 and a_2 spans a plane at the limit vertex and $(\varphi_1, \varphi_2)_j$ is the coordinate of the j -th vertex in C_m^N when we take projection to the tangent plane

$$(3.5.13) \quad \pi: \mathbf{v}_{N_j}^m \mapsto (\varphi_1, \varphi_2)_j.$$

On the other hand, the subdivision can take place on the combinatorial mesh N and generates a domain Ω by the same process we discussed in \mathbb{E}^3 . Thus the corresponding element $v_{N_j}^m$ is equipped with a natural coordinate from Ω

$$(3.5.14) \quad \iota: \mathbf{v}_{N_j}^m \mapsto v_{N_j}^m \in \Omega.$$

Define the transition function

$$(3.5.15) \quad \begin{aligned} \Psi &:= \pi \circ \iota^{-1}: \Omega \rightarrow \text{Span}\{a_1, a_2\} \\ v_{N_j}^m &\mapsto (\varphi_1, \varphi_2)_j \end{aligned},$$

which is also called as the *character map* of the subdivision matrix. Then the smoothness near the limit vertex can be represented by this map. That is, if Ψ is regular, then the limit surface is tangent continuous at the limit vertex, In particular, the limit normal vector $n(\mathbf{v})$ is given as

$$(3.5.16) \quad n(\mathbf{v}) = \frac{a_1 \times a_2}{|a_1 \times a_2|}.$$

Moreover, if Ψ is injective, which infers the injective of the projection π , then the limit surface is single sheeted. Therefore C^1 -continuous.

We end this section by Reif's sufficient condition

Theorem 3.5.6 ([30]). *Let S be a subdivision matrix associated with the invariant neighborhood C_0^N . If the eigenvalue of S satisfies*

$$(3.5.17) \quad 1 = |\lambda_0| > |\lambda_1| = |\lambda_2| \geq \dots \geq |\lambda_{K-1}|$$

and the character map Ψ is regular and injective, then the limit surface generated by S is C^1 -continuous.

Remark 3.5.7.

1. Theorem 3.5.6 provides a sufficient condition for a subdivision algorithm to generate the C^1 -continuous surface.
2. Subdivision algorithm for a discrete surface introduced in Chapter 2 can not be treated by this condition since the topological graph dose not equipped with coordinate.

Chapter 4

Subdivision Algorithms for Trivalent Graphs in \mathbb{E}^3

As we described in the previous section, there exist many types of subdivision schemes with typical features and different valuable advantages. The subdivision zoo in the last chapter introduces some “well-behavior” subdivision algorithms, where we mean by “behavior” the convergent properties. However, one should notice that, so far these subdivision algorithms which produce C^1 (normal)-convergence or C^2 (curvature)-convergence even C^k -convergence, are all established by generating sequences of triangular or square meshes. These specific characters allow for a local parameterization and reasonable combinatorial structures. Classical researches on the limit surfaces, especially the regularity usually regarded in the parameterization near the extraordinary vertices, take plenty of advantages from these standard textures. Furthermore, nowadays one can see a wide exploitation of the triangulations and quadrilaterals in the area of computer graphics, animation industries and engineering designs by the application of geometry processing.

In our work, we concentrate on a new discrete object with a special structure, that is, the trivalent graph in three dimensional Euclidean space. The local trivalent structure provides an intuitive description of the geometries and leads to several natural definitions of geometric quantities which has already been introduced in Chapter 2. A discrete surface under this setting can be described as a combination of finite copies of the basic unit $\tau = (v, E_v)$ equipped with some proper connectivities. One direct observation of this definition is that the discrete surface is no longer a two-dimensional polyhedra, however, a discrete object (vertices) with an indication of interaction noted by edges. General discussions on subdivision schemes in Chapter 3, which extends the area of regular faces to “filling” the “gaps” by the iteration of subdivision processing, may not work effectively. Neither nor the smoothness analysis of the limit surface, which depends on the parameterization method (J. Stam [34]) of the combinatorial mesh with induced coordinate from \mathbb{R}^2 .

In this chapter, we will introduce a specific subdivision algorithm for the trivalent graphs which preserving the local trivalent structure and generating a sequence of convergent subdivisions. In fact, an intuitive understanding of the subdivision algorithms, directly perceived through sense, is given as follows: *generating a sequence of shrinking rings*.

In general, to construct a subdivision algorithm is to describe how to proceed with the algorithm in each step. By the discussions in Chapter 3, each step is obtained by

applying a set of operators on the corresponding invariant neighborhoods, which we call “generating shrinking rings”. This set of operators from every step is consisting of two types, the refinement operator and the smoothing operator. The refinement operator always applying on the combinatorial mesh so that one can insert new elements with corresponding combinatorial information. On the other hand, the smoothing operator assigns the geometric positions to the newly inserted elements, mainly the set of new vertices, and derive a finer control net from the previous one.

In our construction, we firstly introduce a specific refinement operator for topological trivalent graphs, which is called as *Goldberg-Coxeter construction* provided by M. Deza and M. Detour Sikirić [6]. Instead of subdividing the trivalent graph on a plane directly, they consider the subdivision of the dual graph, which turns out to be a triangular mesh. By edge splitting of each triangle, one can obtain a finer triangular mesh whose dual is the refinement of the initial trivalent graph. It should be noted that this construction can be applied to the planar graph only. In our case, we use it ring-wise in the process. Secondly, we define the smoothing operators for each ring and give the geometric positions of the newly inserted vertices. In [13], the smoothing operators for each step of subdivision algorithm are given in a global view, that is, by the *standard realization* (M. Kotani and T. Sunada [16]) of the entire subdivided trivalent graph. Even though a sequence of subdivided discrete surfaces can be produced by this method, the relations between two adjacent steps are not explicit. Therefore the convergent properties are hard to analyzed. In order to improve their method, we provide the smoothing operator by solving a Dirichlet problem with the vertices in each ring of the previous surface as the boundary condition and find the least energy configuration of the corresponding generated ring.

4.1 Goldberg-Coxeter construction of trivalent graphs

The Goldberg-Coxeter construction (GC-construction) is a way to subdivide a planar trivalent graph defined by M. Deza and M. Detour Sikirić [6]. Since the duality relationship between the basic unit and the triangle, this construction provides a successful subdivision method which preserves the trivalent structure.

Definition 4.1.1 (Goldberg-Coxeter construction). Let $X = (V, E)$ be a planar trivalent graph. The graph $GC(X)$ is built in the following steps (see Figure 4.1).

1. Take the dual graph X^* of X . Since X is trivalent, X^* is a triangulation, namely, a plane graph whose faces are all triangles.
2. Every triangle in X^* is subdivided into another set of faces. If we obtain a face which are not triangle, then it can be glued with other neighboring non-triangle faces to form triangles.
3. By duality, the triangulation of (2) is transformed into $GC(X)$.

Now we describe this construction in the view of subdivision algorithm. That is, to generate the sequence of shrinking rings, we need to apply the GC-construction on each ring structure of the given topological trivalent graph. To be more precise, let $X =$

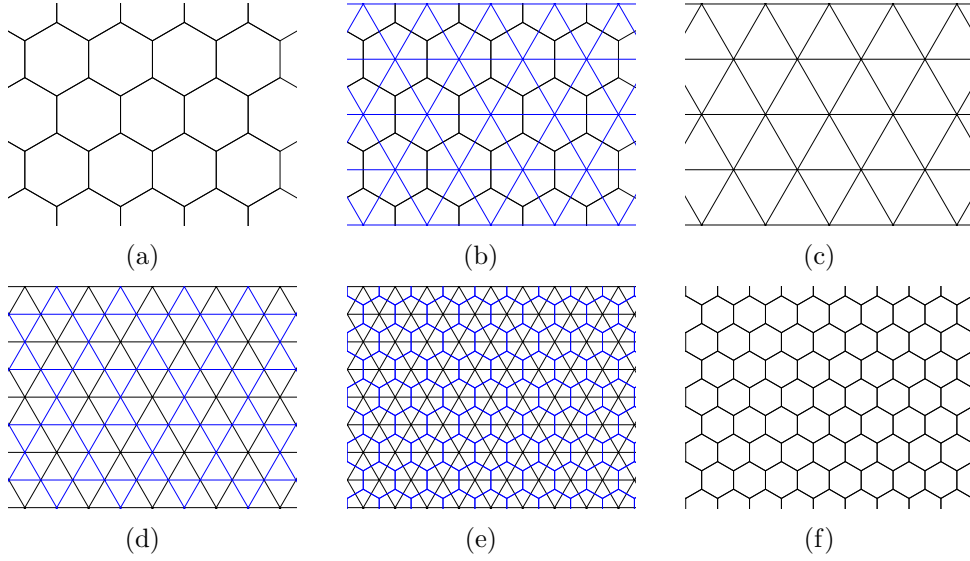


Figure 4.1: the GC-construction of the hexagonal lattice: For a given trivalent graph (a), its dual graph (c) is constructed as shown in (b). The subdivision of (c) is obtained as (d) and its dual graph, (f) is constructed as shown in (e).

(V, E, R) be a trivalent graph in Chapter 2, for an n -ring $r = \{v_0, v_1, \dots, v_{n-1}\} \in R$, we define the *augment n -ring* \tilde{r} by

$$(4.1.1) \quad \tilde{r} := \{\tau_0, \tau_1, \dots, \tau_{n-1}\}$$

where $\tau_i = (v_i, E_{v_i})$ refers to the basic unit centered at v_i (see Figure 4.2(a)).

After an individual step of applying the GC-construction on a fixed augment n -ring \tilde{r} , the edges of r are replaced by 6-rings thus we obtained a small n -ring with n 6-rings as its one-neighborhood. Iteration of the same processing generates the sequences of shrinking rings corresponding to each initial ring. Taking a global version, we finally have a sequence of topological subdivisions X_i of X *ring-wisely*.

Remark 4.1.2.

1. In the present thesis, only $\text{GC}_{2,0}$ (GC-construction of type $(2, 0)$) is utilized to subdivide a topological graph and denoted by GC for simplicity. For more general theory on GC-constructions, please see [6].
2. Since individual edge is replaced by 6-ring after one step of subdivision. Iterated GC-constructions only enlarge the number of 6-rings of the trivalent graph. It does not change the number of the rings in other size. More precisely, on a fixed augment n -ring \tilde{r} , we obtain an n -ring r' in it with n 6-rings as its one-neighborhood after one step of GC-construction. (see Figure 4.2).
3. The limit metric on the domain is not the Euclidean metric but a similar metric studied as the tangent cone at the infinity in [15]. In the present thesis, we concern the metric as the induced metric through the realizations from \mathbb{E}^3 .

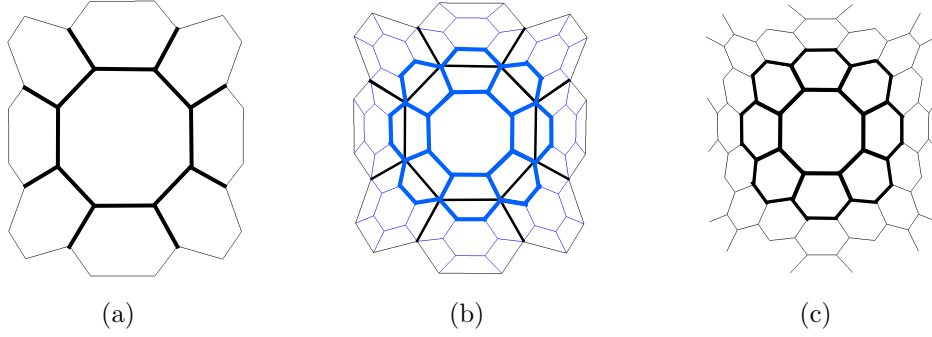


Figure 4.2: Application of the GC-construction to an augment 8-ring (a) (bold line). (b) shows the subdivision process. The result as is shown at (c) is a smaller 8-ring and eight 6-rings as its one-neighborhood (bold line).

4.2 Invariant neighborhood and subdivision matrix

As we mentioned in Chapter 3, the subdivision algorithm locally effects on a given control net. That is, it can be regarded as a combination of local subdivision maps on the corresponding invariant neighborhoods. With the GC-construction as the refinement operator, we are now trying to define a corresponding smoothing operator, which assigns the geometric position to the generated shrinking rings. Since GC-construction is applied on a topological graph *ring-wisely*, the corresponding smoothing operator should follow the same procedure, which means each invariant neighborhood should take the individual ring as its central part.

Given a discrete surface $\Phi: X \rightarrow \mathbb{E}^3$ with $\mathcal{M} = \Phi(X)$. Let

$$(4.2.1) \quad r = \{v_0, v_1, \dots, v_{n-1}\}$$

be an n -ring in R and

$$(4.2.2) \quad r' = \{v'_0, v'_1, \dots, v'_{n-1}\}$$

be the generated n -ring of r after one step of the GC-construction.

We assign the geometry positions for the generated ring. The realization Φ' of r' in \mathbb{E}^3 is given by solving a Dirichlet problem with $V(r)$ as the boundary condition and find the least energy of the augment generated n -ring \tilde{r}' (see Figure 4.3), that is,

$$(4.2.3) \quad E_D(\Phi'(\tilde{r}')) = \min\{\Phi: r' \rightarrow \mathbb{E}^3\}.$$

Let \mathbf{r} and \mathbf{r}' be the corresponding images in \mathbb{E}^3 . When no ambiguity is possible, we identified \mathbf{r} and \mathbf{r}' with their matrix forms respectively. That is,

$$(4.2.4) \quad \mathbf{r} = (\mathbf{v}_0, \mathbf{v}_1, \dots, \mathbf{v}_{n-1})^t \in M(n, 3),$$

$$(4.2.5) \quad \mathbf{r}' = (\mathbf{v}'_0, \mathbf{v}'_1, \dots, \mathbf{v}'_{n-1})^t \in M(n, 3).$$

By the discussion in Chapter 2, the requirement of minimizing of Dirichlet energy equivalent to the balance condition at each newly inserted vertex. That is,

$$(4.2.6) \quad -\mathbf{v}'_{i-1} + 3\mathbf{v}'_i - \mathbf{v}'_{i+1} = \mathbf{v}_i, \quad \text{for } i \in \mathbb{Z}_n.$$

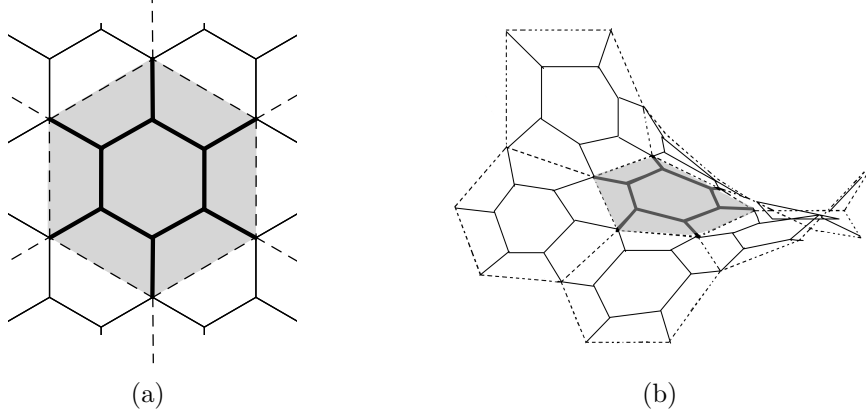


Figure 4.3: (a) shows r (dashed line) and r' (bold line). (b) shows the realization of r (dash line) and r' (bold line) in \mathbb{E}^3 . (Corresponding to the area in shadow.)

Thus the linear relation between \mathbf{r} and \mathbf{r}' is given by

$$(4.2.7) \quad \begin{pmatrix} \mathbf{v}'_0 \\ \mathbf{v}'_1 \\ \mathbf{v}'_2 \\ \mathbf{v}'_3 \\ \dots \\ \mathbf{v}'_{n-1} \end{pmatrix} = \begin{pmatrix} 3 & -1 & 0 & \dots & 0 & -1 \\ -1 & 3 & -1 & \dots & 0 & 0 \\ 0 & -1 & 3 & \dots & 0 & 0 \\ 0 & 0 & -1 & \dots & 0 & 0 \\ & & & \dots & & \\ 0 & 0 & 0 & \dots & 3 & -1 \\ -1 & 0 & 0 & \dots & -1 & 3 \end{pmatrix}^{-1} \begin{pmatrix} \mathbf{v}_0 \\ \mathbf{v}_1 \\ \mathbf{v}_2 \\ \mathbf{v}_3 \\ \dots \\ \mathbf{v}_{n-1} \end{pmatrix}.$$

In particular the corresponding subdivision matrix $S(n)$ of the fixed n -ring is given as

$$(4.2.8) \quad S(n) := \begin{pmatrix} 3 & -1 & 0 & \dots & 0 & -1 \\ -1 & 3 & -1 & \dots & 0 & 0 \\ 0 & -1 & 3 & \dots & 0 & 0 \\ 0 & 0 & -1 & \dots & 0 & 0 \\ & & & \dots & & \\ 0 & 0 & 0 & \dots & 3 & -1 \\ -1 & 0 & 0 & \dots & -1 & 3 \end{pmatrix}^{-1} \in M(n),$$

and the eigenvalues of $S(n)$ are

$$(4.2.9) \quad \lambda_k(n) = \frac{1}{1 + 4 \sin^2(k\pi/n)}, \quad k \in \mathbb{Z}_n.$$

Therefore by the discussion in Chapter 3, this local subdivision map corresponding to n -ring as the invariant neighborhood is converged since

$$(4.2.10) \quad 1 = \lambda_0(n) > \lambda_1(n) \geq \lambda_2(n) \geq \dots \geq \lambda_{n-1}(n).$$

4.3 GC-subdivision of discrete surfaces

Now we begin to construct a subdivision algorithm based on the subdivision matrices we defined on each ring above. In [37], we use the matrices directly for each ring and established an interpolate subdivision algorithm. The convergence seems obvious, however, it

generates a large number of singularities in the numerical experiments in the last Chapter. We improve this original algorithm by modifications on specific vertices and construct the modified subdivision algorithm.

Let $X_0 = (V_0, E_0, R_0)$ be a topological trivalent graph and X_{i+1} be the GC-construction of X_i , i.e., $X_{i+1} := \text{GC}(X_i)$, for any $i \in \mathbb{N}$.

Assume we have already obtained

$$(4.3.1) \quad \Phi_i: X_i \rightarrow \mathbb{E}^3 \text{ with } \mathcal{M}_i = \Phi(X_i),$$

and define

$$(4.3.2) \quad \Phi'_{i+1}: X_{i+1} \rightarrow \mathbb{E}^3 \text{ with } \mathcal{M}'_{i+1} = \Phi'(X_{i+1})$$

as a minimizing map of the Dirichlet energy from X_{i+1} with $\mathcal{M}_i = \Phi_i(X_i)$ as the boundary condition, namely it satisfies

1. $\Phi'_{i+1}(V_i) = \Phi_i(V_i)$,
2. Φ'_{i+1} takes the minimum of the Dirichlet energy in local, i.e., for any fixed ring $r^i \in R_i$ and the associated generated ring $r^{i+1} \in R_{i+1}$,

$$(4.3.3) \quad E_D(\Phi'_{i+1}(\tilde{r}^{i+1})) = \min\{E_D(\Phi': \tilde{r}^{i+1} \rightarrow \mathbb{E}^3)\}.$$

The vertices set \mathcal{V}'_{i+1} of \mathcal{M}'_{i+1} is a union of two disjoint sets, i.e., $\mathcal{V}'_{i+1} = \mathcal{V}_i \cup \mathcal{V}^i_{i+1}$, where $\mathcal{V}_i = \Phi_i(V_i)$ and \mathcal{V}^i_{i+1} is the set of solution vertices of the boundary problem. However, the connectivity of the vertices is reconstructed by the corresponding relations in X_{i+1} .

Define a projection

$$(4.3.4) \quad \pi_{i+1}: \mathcal{M}'_{i+1} \rightarrow \mathbb{E}^3$$

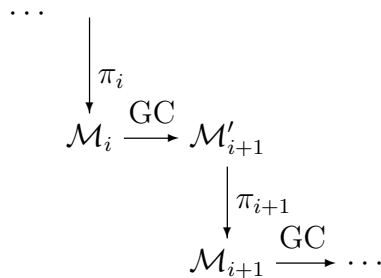
with \mathcal{M}_{i+1} as the image. For any $\mathbf{v} \in \mathcal{M}'_{i+1}$

$$(4.3.5) \quad \pi_{i+1}(\mathbf{v}) = \begin{cases} \mathbf{v} & \mathbf{v} \in \mathcal{V}^i_{i+1} \\ \text{barycenter of its neighbors} & \mathbf{v} \in \mathcal{V}_i \end{cases}.$$

Finally, let

$$(4.3.6) \quad \Phi_{i+1} = \pi_{i+1} \circ \Phi'_{i+1}: X_{i+1} \rightarrow \mathbb{E}^3, \text{ with } \mathcal{M}_{i+1} = \Phi(X_{i+1}).$$

Then we construct a subdivision algorithm which generates a sequence of discrete surfaces $\{\mathcal{M}_i\}_i$ by the iterative processing shown as the following diagram



Remark 4.3.1.

1. Since the subdivision algorithm is established by modification of the original method in [37], the invariant neighborhoods and corresponding subdivision matrices are also changed. We address a proof of the convergence based on the analysis of Dirichlet energy in next chapter.
2. The comparison of these two algorithms will list in the numerical experiments in the last chapter.

Chapter 5

Evaluation and estimate

In classical subdivision theory, discussions of the regularity of the limit surface often require the existence of smooth parameterization of this limit. The locality of subdivision algorithms suggests that the processes reproduce the initial control nets by applying particular subdivision matrices on corresponding invariant neighborhoods iteratively. Thus the spectrum of the subdivision matrices indicate the convergent properties of the global subdivision algorithms. In the polyhedral mesh case, for example, the combinatorial mesh of a triangular mesh can be treated as a triangulation of a parameterized domain in \mathbb{R}^2 , which can also provide a parameterization of its image as the discrete surface in \mathbb{R}^3 . Most of the subdivision algorithms take advantages from these specific structures.

In our work, however, the discrete surface is given as a realization of a topological trivalent graph. One of the fundamental problems is how to discuss the convergence and the regularity of the subdivision algorithm without parameterizations of the combinatorial mesh. In this chapter, we consider this problem in the view of the Dirichlet energy and provide proof of the convergence of the modified subdivision algorithm by discussing the local behavior of the Dirichlet energy. Furthermore, we discuss the limit of the subdivision sequence and prove the monotonicity of the Dirichlet energy which is determined by the topology of the initial discrete surface.

5.1 Convergence of the modified subdivision algorithm

Individual step of a given subdivision algorithm is applied on a particular ring and its neighborhood. We firstly introduce the discussion on the monotonicity of the Dirichlet energy of adjacent two steps from the original subdivision method in [37].

Proposition 5.1.1 ([37]). *For any n -ring r and the associated n -ring r' which generated by one step of the GC-construction, there exists a constant number $\lambda(n) < 1$ such that*

$$(5.1.1) \quad E_D(\Phi'(\tilde{r}')) \leq \lambda(n) E_D(\Phi(r)),$$

where \tilde{r}' is the augmented n -ring of r' .

Proof. Let \mathbf{r} and \mathbf{r}' be the corresponding images of r and r' in \mathbb{E}^3 . When no ambiguity is possible, we identified \mathbf{r} and \mathbf{r}' with their matrix forms respectively. That is,

$$(5.1.2) \quad \mathbf{r} = (\mathbf{v}_0, \mathbf{v}_1, \dots, \mathbf{v}_{n-1})^t \in M(n, 3)$$

$$(5.1.3) \quad \mathbf{r}' = (\mathbf{v}'_0, \mathbf{v}'_1, \dots, \mathbf{v}'_{n-1})^t \in M(n, 3)$$

where \mathbf{v}_0 and \mathbf{v}'_0 are connected by a single edge.

Then Dirichlet energy of \mathbf{r} and $\tilde{\mathbf{r}}'$ can be represented as the following, respectively

$$(5.1.4) \quad E_D(\Phi'(\tilde{\mathbf{r}}')) = \sum_{i=0}^{n-1} |\mathbf{v}_i - \mathbf{v}'_i|^2 + \sum_{i=0}^{n-1} |\mathbf{v}'_i - \mathbf{v}'_{i+1}|^2 = \|\mathbf{r} - \mathbf{r}'\|^2 + \|\mathbf{r}' - T\mathbf{r}'\|^2,$$

$$(5.1.5) \quad E_D(\Phi(r)) = \sum_{i=0}^{n-1} |\mathbf{v}_i - \mathbf{v}_{i+1}|^2 = \|\mathbf{r} - T\mathbf{r}\|^2,$$

where $|\cdot|$ is the vector norm, $\|\cdot\|$ is the Hilbert-Schmidt norm of the square matrix and T is the matrix operator that exchanges the order of the rows

$$(5.1.6) \quad T := \begin{pmatrix} O & I_{n-1} \\ 1 & O^T \end{pmatrix} \in M(n).$$

The the requirement of minimizing the Dirichlet energy equivalent to the balancing condition at each inserted vertex, in fact

$$(5.1.7) \quad \frac{\partial E_D(\Phi'(\tilde{\mathbf{r}}'))}{\partial \mathbf{v}'_i} = 0, \quad \text{for } i \in \mathbb{Z}_n,$$

which is

$$(5.1.8) \quad -\mathbf{v}'_{i-1} + 3\mathbf{v}'_i - \mathbf{v}'_{i+1} = \mathbf{v}_i, \quad \text{for } i \in \mathbb{Z}_n.$$

Then we obtain the linear relationship between \mathbf{r} and the associated \mathbf{r}' as following

$$(5.1.9) \quad \mathbf{r}' = S(n)\mathbf{r},$$

where

$$(5.1.10) \quad S(n) := (3I_n - T - T^t)^{-1} = \begin{pmatrix} 3 & -1 & 0 & \dots & 0 & -1 \\ -1 & 3 & -1 & \dots & 0 & 0 \\ 0 & -1 & 3 & \dots & 0 & 0 \\ 0 & 0 & -1 & \dots & 0 & 0 \\ & & & \dots & & \\ 0 & 0 & 0 & \dots & 3 & -1 \\ -1 & 0 & 0 & \dots & -1 & 3 \end{pmatrix}^{-1} \in M(n),$$

and I_n is the identity matrix of size n .

Direct computation shows the eigenvalue of $S(n)$ as following

$$(5.1.11) \quad \lambda_k(n) = \frac{1}{1 + 4 \sin^2(k\pi/n)}, \quad k \in \mathbb{Z}_n.$$

On the other hand, since $S(n)$ is symmetric, we have the following equation

$$(5.1.12) \quad S(n)(\mathbf{r} - T\mathbf{r}) = S(n)\mathbf{r} - S(n)T\mathbf{r} = S(n)\mathbf{r} - TS(n)\mathbf{r} = \mathbf{r}' - T\mathbf{r}'.$$

Here we claim that

$$(5.1.13) \quad \mathbf{r} - T\mathbf{r} \perp \phi_0, \quad \mathbf{r}' - T\mathbf{r}' \perp \phi_0,$$

where $\varphi_0 = (1, \dots, 1)^T$ is the eigenvector of $\lambda_0 = 1$.

In fact, if we let $\mathbf{r} = c^0\varphi_0 + \mathbf{r}_\perp$, where $\mathbf{r}_\perp \perp \varphi_0$. By noticing that $T\varphi_0 = \varphi_0$, we have

$$(5.1.14) \quad \begin{aligned} \langle \mathbf{r} - T\mathbf{r}, \varphi_0 \rangle &= \langle \mathbf{r}_\perp - T\mathbf{r}_\perp, \varphi_0 \rangle = \langle \mathbf{r}_\perp, \varphi_0 \rangle - \langle T\mathbf{r}_\perp, \varphi_0 \rangle \\ &= -\langle T\mathbf{r}_\perp, T\varphi_0 \rangle = -T\langle \mathbf{r}_\perp, \varphi_0 \rangle \\ &= 0. \end{aligned}$$

Similarly, we can also prove $\mathbf{r}' - T\mathbf{r}' \perp \varphi_0$ by noticing the fact that

$$(5.1.15) \quad S(n)\varphi_0 = \lambda_0(n)\varphi_0 = \varphi_0.$$

Let $\tilde{\sigma}(S(n))$ be the sub-dominate eigenvalue of $S(n)$, by (5.1.13) we have

$$(5.1.16) \quad \|\mathbf{r}' - T\mathbf{r}'\|^2 \leq \tilde{\sigma}(S(n))^2 \|\mathbf{r} - T\mathbf{r}\|^2 = \lambda_1^2(n) \|\mathbf{r} - T\mathbf{r}\|^2.$$

Similarly,

$$(5.1.17) \quad \|\mathbf{r} - \mathbf{r}'\|^2 \leq \lambda_1(n)(1 - \lambda_1(n)) \|\mathbf{r} - T\mathbf{r}\|^2.$$

Therefore

$$\begin{aligned} \|\mathbf{r}' - T\mathbf{r}'\|^2 + \|\mathbf{r} - \mathbf{r}'\|^2 &\leq \lambda_1^2(n) \|\mathbf{r} - T\mathbf{r}\|^2 + \lambda_1(n)(1 - \lambda_1(n)) \|\mathbf{r} - T\mathbf{r}\|^2 \\ &= \lambda_1(n) \|\mathbf{r} - T\mathbf{r}\|^2, \end{aligned}$$

where $\lambda_1(n) = 1/(1 + 4\sin^2(\pi/n)) < 1$ as desired. \square

By using the monotone decreasing of the local Dirichlet energy, we can prove the convergence of modified subdivision algorithm.

Theorem 5.1.2 ([14]). *The sequence of discrete surfaces $\{\mathcal{M}_i\}_{i=0}^\infty$ that are constructed by the modified GC-subdivisions forms a Cauchy sequence in the Hausdorff topology.*

Proof. Let r^i be a fixed n -ring in R_i , r^{i+1} be the associated generated n -ring in R_{i+1} . Now we consider the Hausdorff distance d_H of these rings

$$(5.1.18) \quad \begin{aligned} d_H(\Phi_i(r^i), \Phi'_{i+1}(r^{i+1})) &\leq \sum_{e \in E(r^{i+1})} |\Phi'_{i+1}(e)| \\ &\leq \sqrt{2n(E_D(\Phi'_{i+1}(r^{i+1})))} \leq E_0(n) \sqrt{\lambda_1^{i+1}(n)}, \end{aligned}$$

where $E_0(n) := \sqrt{2nE_D(\Phi_0(r^0))}$ is constant which determined by the initial discrete surface $\Phi_0: X_0 \rightarrow \mathbb{E}^3$ with $\mathcal{M}_0 = \Phi(X_0)$ and $\lambda_1(n) = 1/(1 + 4\sin^2(\pi/n))$. Since each face of a fixed trivalent graph has finite many of edges, that is, n is bounded from above. Let $\lambda_1 = \max\{\lambda_1(n)\}$, $E = \max\{E_0(n)\}$, we have

$$(5.1.19) \quad d_H(\mathcal{M}_i, \mathcal{M}'_{i+1}) = \sup_{r^i \in R_i} \{d_H(\Phi_i(r^i), \Phi'_{i+1}(r^{i+1}))\} \leq E \sqrt{\lambda_1^{i+1}}.$$

On the other hand, take $\mathbf{v} \in \mathbf{r}^i$, also we have $\mathbf{v} \in \mathcal{V}_i$. Since $\pi_{i+1}(\mathbf{v})$ is the barycenter of its nearest neighbors, we have

$$(5.1.20) \quad d_H(\mathbf{v}, \pi_{i+1}(\mathbf{v})) < \sup_{\mathbf{r}^i \in R_i} \{d_H(\Phi_i(\mathbf{r}^i), \Phi'_{i+1}(\mathbf{r}^{i+1}))\} = d_H(\mathcal{M}_i, \mathcal{M}'_{i+1}).$$

That is,

$$(5.1.21) \quad d_H(\mathcal{M}_i, \mathcal{M}_{i+1}) = d_H(\mathcal{M}_i, \pi_{i+1}(\mathcal{M}'_{i+1})) = \sup_{\mathbf{v} \in \mathcal{V}_i} \{d_H(\mathbf{v}, \pi_{i+1}(\mathbf{v}))\} \leq E\sqrt{\lambda_1^{i+1}}.$$

Thus for any $\varepsilon > 0$, let $N = \lceil 2 \log_{1/\lambda_1}(\Lambda/\varepsilon) \rceil$. Then for any $i, j > \mathbb{N}$ ($j > i$), we have

$$\begin{aligned} d_H(\mathcal{M}_i, \mathcal{M}_j) &\leq d_H(\mathcal{M}_i, \mathcal{M}_{i+1}) + d_H(\mathcal{M}_{i+1}, \mathcal{M}_{i+2}) + \cdots + d_H(\mathcal{M}_{j-1}, \mathcal{M}_j) \\ &\leq E \left(\sqrt{\lambda_1^{i+1}} + \sqrt{\lambda_1^{i+2}} + \cdots + \sqrt{\lambda_1^j} \right) \\ &< \Lambda E \sqrt{\lambda_1^{i+1}} \\ &< \varepsilon, \end{aligned}$$

where $\Lambda = (1 + \sqrt{\lambda_1})/(1 - \lambda_1)$ is a constant determined by the initial discrete surface as well. \square

5.2 The limit set of the subdivision sequence

We address a proof of the convergence of the modified subdivision algorithm through the view of Dirichlet energy. In this section, we discuss the limit space.

Let $\mathcal{M}_0 = \{\mathcal{V}_0, \mathcal{E}_0, \mathcal{R}_0\}$ be a trivalent graph in \mathbb{E}^3 and $\{\mathcal{M}_i\}_{i=0}^\infty = \{\mathcal{V}_i, \mathcal{E}_i, \mathcal{R}_i\}_{i=0}^\infty$ be the sequence constructed by the modified GC-subdivision. The limit set \mathcal{M}_∞ of this sequence in the Hausdorff topology is divided into three types:

$$\mathcal{M}_\infty = \mathcal{M}_\mathcal{R} \cup \mathcal{M}_\mathcal{V} \cup \mathcal{M}_\mathcal{S}.$$

The first two come from accumulating vertices of the shrinking invariant neighborhoods and the third one emerges as a global accumulation.

More precisely, $\mathcal{M}_\mathcal{R}$ is the set of accumulating vertices associated with each ring in \mathcal{M}_i . We have the following proposition

Proposition 5.2.1.

$$(5.2.1) \quad \mathcal{M}_\mathcal{R} := \bigcup_i \{ \text{the barycenters of all rings } \mathbf{r}^i \in \mathcal{M}_i \}.$$

Lemma 5.2.2. *For any n -ring $\mathbf{r}^i \in \mathcal{R}_i$, let $\mathbf{r}^{i+1} = S(n) \cdot \mathbf{r}^i$. Then we have*

$$\mathbf{r}^{i+1} \subset \text{conv}(\mathbf{r}^i),$$

where $S(n)$ is the subdivision matrix and $\text{conv}(\underline{\cdot})$ means the convex hull of the corresponding object $\underline{\cdot}$.

Proof. Let $S(n) = (a_{lm})_{lm}$ ($l, m \in \mathbb{Z}_n$), $\mathbf{r}^i = (\mathbf{v}_0^i, \mathbf{v}_1^i, \dots, \mathbf{v}_{n-1}^i)^t$. Noticed that $S(n) \cdot \mathbf{1} = \mathbf{1}$, then for any l

$$(5.2.2) \quad \sum_{m=0}^{n-1} a_{lm} \mathbf{v}_m^i = \mathbf{v}_l^{i+1},$$

where

$$(5.2.3) \quad \sum_{m=0}^{n-1} a_{lm} = 1, \quad a_{lm} \geq 0.$$

That is,

$$\mathbf{r}^{i+1} \subset \text{conv}(\mathbf{r}^i).$$

□

It also shows that \mathbf{r}^i and \mathbf{r}^{i+1} share one same barycenter \mathbf{r}^b . Furthermore, since $\mathbf{r}^{(i+k)} = S_n^k \cdot \mathbf{r}^i$, by Proposition 5.1.1

$$(5.2.4) \quad E_D(\mathbf{r}^{(i+k)}) < \lambda_1^k \cdot E_D(\mathbf{r}^i) \rightarrow 0 \text{ as } k \rightarrow \infty,$$

which means \mathbf{r}^i degenerates to a single vertex as i goes to ∞ . We call this point \mathbf{r}^∞ as the accumulate point associated with \mathbf{r}^i . Easy to see for any k , \mathbf{r}^∞ and \mathbf{r}^b are lying in the same convex hull of $\mathbf{r}^{(i+k)}$. Therefore $\mathbf{r}^\infty = \mathbf{r}^b$ complete the proof of Proposition 5.2.1.

A corollary direct from the Proposition 5.2.1 as a consequence.

Corollary 5.2.3. *Any fixed n -ring of the discrete surface will converge to its barycenter by the GC-subdivision. Further more, the convergence rate varies inversely with n .*

On the other hand, \mathcal{M}_V is the set of all inserted vertices. The convergence to a vertex in \mathcal{M}_V is pathological, although we have the energy monotonicity formula (Theorem 5.3.2). It seems the balancing condition plays an important role.

For example, when we take the atomic configuration of the fullerene C_{60} , a polygonal graph on the sphere, which does not satisfy the balancing condition, we obtain a pathological shape as the limit of its subdivisions. It seems the modified method gives a better convergent than the original method in [37]. For numerical calculations for C_{60} , Mackay crystal of type P and their subdivision, see Chapter 6.

So far, for a general discrete surface \mathcal{M} , we know little about the set \mathcal{M}_S of the limit of the subdivision sequence which constructed by the GC-subdivision. Under a natural condition, however, we prove \mathcal{M}_S is empty.

We introduce a definition of a specific discrete surface as following: \mathcal{M} is said to be *un-branched* if each edge is shared by two rings. One of the examples of *branched* discrete surfaces is discussed in [14].

Theorem 5.2.4 ([14]). *Let $\mathcal{M}_0 = \{\mathcal{V}_0, \mathcal{E}_0, \mathcal{R}_0\}$ be a trivalent graph in \mathbb{E}^3 satisfies*

1. *Each edge of \mathcal{M}_0 is shared by two rings at most.*
2. *Any two rings intersect at one edge or empty.*

3. For any two n -rings \mathbf{r}_i and $\mathbf{r}_j \in \mathcal{R}_0$, the convex hull $\text{conv}(\mathcal{N}(\mathbf{r}_i))$ of the one-neighborhood $\mathcal{N}(\mathbf{r}_i)$ of \mathbf{r}_i and the convex hull $\text{conv}(\mathcal{N}(\mathbf{r}_j))$ of the one-neighborhood $\mathcal{N}(\mathbf{r}_j)$ of \mathbf{r}_j intersect when either \mathbf{r}_i and \mathbf{r}_j share a common edge or there is a ring $\mathbf{r}_i \diamond \mathbf{r}_j$ as the common one-neighbor of \mathbf{r}_i and \mathbf{r}_j .

Then $\mathcal{M}_\infty = \mathcal{M}_\mathcal{V} \cup \mathcal{M}_\mathcal{R}$.

We prove Theorem 5.2.4 by the followings. An one-neighborhood of an n -ring \mathbf{r} is a set

$$\mathcal{N}(\mathbf{r}) = \{\mathbf{r}, \mathbf{r}_1, \mathbf{r}_2, \dots, \mathbf{r}_n\}$$

of \mathbf{r} and its one-neighbor rings \mathbf{r}_α , $\alpha \in \{1, 2, \dots, n\}$. We firstly consider the following Lemma

Lemma 5.2.5.

$$\bigcup_{\mathbf{r}^{i+1} \in \mathcal{R}_{i+1}} \text{conv}(\mathcal{N}(\mathbf{r}^{i+1})) \subset \bigcup_{\mathbf{r}^i \in \mathcal{R}_i} \text{conv}(\mathcal{N}(\mathbf{r}^i)),$$

Proof. Noticing that in one individual subdividing process, we have two kinds of rings. One is the generated rings which obtained as a solution \mathbf{r}' of the Dirichlet problem with the boundary condition \mathbf{r} by the equation (5.1.9). That is

$$\mathbf{r}' = S \cdot \mathbf{r},$$

and the one-neighborhood of \mathbf{r}' is given as

$$\mathcal{N}(\mathbf{r}') = \{\mathbf{r}', \mathbf{r}' \diamond \mathbf{r}'_1, \dots, \mathbf{r}' \diamond \mathbf{r}'_n\},$$

where $\mathbf{r}' = S \cdot \mathbf{r}$ and $\mathbf{r}'_\alpha = S \cdot (\mathbf{r}_\alpha)$ ($\alpha \in \{1, \dots, n\}$) although we use the same S to show the linear relations, however, the size of S is depending on the size of the ring that applied on. The other one is the common one-neighboring 6-ring of two rings \mathbf{r}' and \mathbf{r}'_α ($\alpha \in \{1, \dots, n\}$). We denote it as $\mathbf{r}' \diamond \mathbf{r}'_\alpha$. Since we identity each ring with the set of its vertices, we have

$$\mathbf{r}' \diamond \mathbf{r}'_\alpha \subset \mathbf{r}' \cup \mathbf{r}'_\alpha \cup \mathbf{r} = S \cdot \mathbf{r} \cup S \cdot \mathbf{r}_\alpha \cup \pi(\mathbf{r}),$$

and the one-neighborhood of $\mathbf{r}' \diamond \mathbf{r}'_\alpha$ is given as

$$\mathcal{N}(\mathbf{r}' \diamond \mathbf{r}'_\alpha) = \{\mathbf{r}' \diamond \mathbf{r}'_\alpha, \mathbf{r}', \mathbf{r}'_\alpha, \mathbf{r}' \diamond \mathbf{r}'_{\alpha-1}, \mathbf{r}' \diamond \mathbf{r}'_{\alpha+1}, \mathbf{r}'_\alpha \diamond \mathbf{r}'_{\alpha-1}, \mathbf{r}'_\alpha \diamond \mathbf{r}'_{\alpha+1}\}.$$

Notice for a given $\mathbf{R} \in \mathcal{R}_{i+1}$, there is a face $\mathbf{r} \in \mathcal{R}_i$ such that $\mathbf{R} \in \mathcal{N}(\mathbf{r})$. More precisely \mathbf{R} is either a solution ring $\mathbf{r}' = S \cdot \mathbf{r}$ or a common one-neighboring ring $\mathbf{r}' \diamond \mathbf{r}'_\alpha$.

In the case that $\mathbf{R} = \mathbf{r}' = S \cdot \mathbf{r}$ in \mathcal{R}_{i+1} with $\mathbf{r} \in \mathcal{R}_i$, we have $\text{conv}(\mathcal{N}(\mathbf{R})) \subset \text{conv}(\mathcal{N}(\mathbf{r}))$. Since we have the relation

$$\mathcal{N}(\mathbf{r}) \subset S \cdot \mathbf{r} \bigcup \bigcup_\alpha S \cdot \mathbf{r}_\alpha \bigcup \pi(\mathbf{r}),$$

where π is the action of taking the barycenter of the three nearest neighboring vertices. They are all linear combination of elements of $\mathcal{N}(\mathbf{r})$, and this relation yields the claim.

In the case that $\mathbf{R} = \mathbf{r}' \diamond \mathbf{r}'_\alpha$ in \mathcal{M}_{i+1} with $\mathbf{r} \in \mathcal{M}_i$ and an one-neighboring ring \mathbf{r}_α of \mathbf{r} ,

$$\text{conv}(\mathcal{N}(\mathbf{R})) \subset \text{conv}(\mathcal{N}(\mathbf{r})) \cup \text{conv}(\mathcal{N}(\mathbf{r}_\alpha)).$$

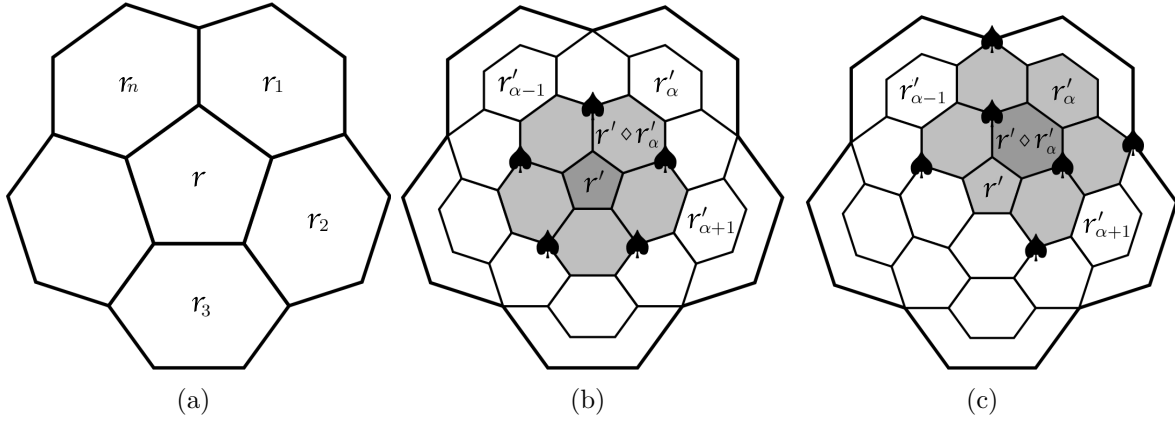


Figure 5.1: (a) $\mathcal{N}(\mathbf{r}) = \{\mathbf{r}, \mathbf{r}_1, \dots, \mathbf{r}_n\}$, (b) the gray face and light-gray faces consists $\mathcal{N}(\mathbf{r}')$, (c) the gray face and light-gray faces consists $\mathcal{N}(\mathbf{r}' \diamond \mathbf{r}'_\alpha)$ (♠ refers to the projection).

We also have the relation

$$\mathcal{N}(\mathbf{R}) \subset \pi(\mathbf{r}) \cup \pi(\mathbf{r}_\alpha) \cup S \cdot \mathbf{r} \cup S \cdot \mathbf{r}_\alpha \cup S \cdot \mathbf{r}_{\alpha-1} \cup S \cdot \mathbf{r}_{\alpha+1},$$

where π is the action of taking the barycenter of the three nearest neighboring vertices, and here we use the vertices of $\mathcal{N}(\mathbf{r}_\alpha)$ only. Therefore elements in $\mathcal{N}(\mathbf{R})$ are again all linear combination of elements of $\mathcal{N}(\mathbf{r})$ and $\mathcal{N}(\mathbf{r}_\alpha)$.

Combining these two cases we have

$$\bigcup_{\mathbf{r}^{i+1} \in \mathcal{R}_{i+1}} \text{conv}(\mathcal{N}(\mathbf{r}^{i+1})) \subset \bigcup_{\mathbf{r}^i \in \mathcal{R}_i} \text{conv}(\mathcal{N}(\mathbf{r}^i)).$$

□

We define

$$\mathcal{C}_i := \bigcup_{\mathbf{r} \in \mathcal{R}_i} \text{conv}(\mathcal{N}(\mathbf{r})).$$

The lemma claims

$$\mathcal{M}_\infty \subset \dots \subset \mathcal{C}_{i+1} \subset \mathcal{C}_i \subset \dots \mathcal{C}_0.$$

In particular, for any $\mathbf{v}^\infty \in \mathcal{M}_\infty$, assume that $\mathbf{v}^\infty \notin \mathcal{M}_\mathcal{V}$ and take a sequence of vertices \mathbf{v}^k such that $\lim \mathbf{v}^k = \mathbf{v}^\infty$. Since $\mathbf{r}^\infty \notin \mathcal{M}_\mathcal{V}$, we assume no two \mathbf{v}^k and \mathbf{v}^j are in the same stage, i.e., there is a unique $\mathbf{v}^i \in \mathcal{R}_i$ for every i without loss of generality.

Let $\mathbf{v}^i \in \mathbf{r}^i$ and $\mathbf{v}^{i+1} \in \mathbf{r}^{i+1}$, then we have

$$\mathbf{r}^{i+1} = S \cdot \mathbf{r}^i$$

or

$$\mathbf{r}^{i+1} = S \cdot \mathbf{r}^i \diamond S \cdot \mathbf{r}_\alpha^i$$

where \mathbf{r}^i and \mathbf{r}_α^i are two neighbored rings in \mathcal{R}_i . Since we assume two convex hulls of one-neighborhoods $\mathcal{N}(\mathbf{r})$ and $\mathcal{N}(\mathbf{r}_\alpha)$ intersect only when \mathbf{r} and \mathbf{r}_α adjacent or there is a common one-neighboring ring $\mathbf{r} \diamond \mathbf{r}_\alpha$.

In the latter case, $\mathbf{v}^{i+1} \in \mathbf{r}^i \cap \mathbf{r}_\alpha^i$ which contradicts the choice of the sequence. Therefore

$$\mathbf{v}^{i+1} \in S \cdot \mathbf{r}^i \quad \text{with } \mathbf{v}^i \in \mathbf{r}^i.$$

That implies \mathbf{v}^∞ is the accumulate point of a ring, that is, $\mathbf{v}^\infty \in \mathcal{M}_\mathcal{R}$, and complete the proof of Theorem 5.2.4.

5.3 Monotonicity of the Dirichlet energy

Let $\{\mathcal{M}_i\}_i^\infty$ be the sequence of discrete surfaces with $\mathcal{M}_i = (\mathcal{V}_i, \mathcal{E}_i, \mathcal{R}_i)$ as the discrete surface of the i -th step constructed from an un-branched initial discrete surface \mathcal{M}_0 . Now we show the monotonicity of the Dirichlet energy.

For a given n -ring, individual step of the GC-construction of the topological trivalent graph generates a smaller n -ring and reconstructs the neighbor combination such that each edge from the previous graph is replaced by a 6-ring. Therefore even the size of the ring set keep enlarging when the subdivision process applied iterated, however, the number of n -ring with $n \neq 6$ remains constant. This observation provides the core idea for the following proof.

Let \mathcal{R}_i be the set of rings from the i -th step of construction. \mathcal{R}_i is a union of three disjoint sets of rings, that is

$$(5.3.1) \quad \mathcal{R}_i = \mathcal{R}_i^{n<6} \bigcup \mathcal{R}_i^{n=6} \bigcup \mathcal{R}_i^{n>6},$$

where n denoted as the size of the rings in each corresponding set. That is, $\mathcal{R}_i^{n=6}$ is the set of 6-rings in \mathcal{M}_i and $\mathcal{R}_i^{n<6}$ and $\mathcal{R}_i^{n>6}$ are the sets of n -rings in \mathcal{M}_i with $n < 6$ and $n > 6$, respectively. Since the initial discrete surface is finite, there exists an N -ring with the largest size N . The GC-subdivision enlarges the size of 6-rings only, we have

$$(5.3.2) \quad \#\mathcal{R}_i^{n<6} = \#\mathcal{R}_0^{n<6}, \quad \#\mathcal{R}_i^{n>6} = \#\mathcal{R}_0^{n>6}.$$

Lemma 5.3.1. *Let \mathbf{r} be an n -ring in \mathcal{M}_i and \mathbf{r}' be the associated n -ring in \mathcal{M}_{i+1} as a solution of the Dirichlet problem with the boundary \mathbf{r} .*

$$(5.3.3) \quad E_D(\mathbf{r}') \leq \lambda_1^2(n) E_D(\mathbf{r}),$$

where $\lambda_1^2(n)$ is the sub-dominant eigenvalue of the subdivision matrix $S(n)$.

Proof. Since the property of GC-subdivision, $\mathbf{r}' = S(n) \cdot \mathbf{r}$. The assertion is obvious. \square

Theorem 5.3.2 (Monotonicity of the Dirichlet energy [14]). *Let $\{\mathcal{M}_i\}_i^\infty$ be the sequence of discrete surfaces constructed from a finite discrete surface \mathcal{M}_0 which at least has one n -ring with $n \neq 6$. The Dirichlet energy of \mathcal{M}_i is bounded from above by the constant independent of n . Moreover, it is monotone decreasing after enough steps if there is no n -ring with $n > 6$, conversely, it is monotone increasing after enough steps if there is no n -ring with $n < 6$.*

Proof. By the definition of Dirichlet energy, we have

$$(5.3.4) \quad E_D(\mathcal{M}_i) = \sum_{e \in \mathcal{E}_i} |e|^2 = \frac{1}{2} \sum_{\mathbf{r}^i \in \mathcal{R}_i} E_D(\mathbf{r}^i).$$

For any $\mathbf{r}^i \in \mathcal{R}_i$, let \mathbf{r}^{i+1} be the associated generated n -ring, i.e., the solution of the Dirichlet problem with the boundary \mathbf{r}^i . Then

$$(5.3.5) \quad E_D(\mathcal{M}_{i+1}) = \sum_{\mathbf{r}^{i+1} = S(n) \cdot \mathbf{r}^i, \mathbf{r}^i \in \mathcal{R}_i} E_D(\tilde{\mathbf{r}}^{i+1}),$$

where $\tilde{\mathbf{r}}^{i+1}$ is the augmented ring of \mathbf{r}^{i+1} . Now we compute the Dirichlet energy of \mathcal{M}_{i+1} ,

$$(5.3.6) \quad \begin{aligned} E_D(\mathcal{M}_{i+1}) &= \sum_{\mathbf{r}^{i+1} = S(n) \cdot \mathbf{r}^i, \mathbf{r}^i \in \mathcal{R}_i} E_D(\tilde{\mathbf{r}}^{i+1}) \\ &\leq \sum_{\mathbf{r}^i \in \mathcal{R}_i} \lambda_1(n) E_D(\mathbf{r}^i) \\ &\leq \frac{1}{2} \sum_{\mathbf{r}^i \in \mathcal{R}_i^{n < 6}} E_D(\mathbf{r}^i) + \frac{1}{2} \sum_{\mathbf{r}^i \in \mathcal{R}_i^{n=6}} E_D(\mathbf{r}^i) + \lambda_1(N) \sum_{\mathbf{r}^i \in \mathcal{R}_i^{n > 6}} E_D(\mathbf{r}^i) \\ &= \frac{1}{2} \sum_{\mathbf{r}^i \in \mathcal{R}_i} E_D(\mathbf{r}^i) + \left(\lambda_1(N) - \frac{1}{2} \right) \sum_{\mathbf{r}^i \in \mathcal{R}_i^{n > 6}} E_D(\mathbf{r}^i). \end{aligned}$$

The first inequality is due to (5.1.1) and the second estimate is due to the inequality

$$(5.3.7) \quad \begin{aligned} \lambda_1(n) &< 1/2 && \text{for } n < 6, \\ \lambda_1(6) &= 1/2, \\ \lambda_1(n) &< \lambda_1(N) && \text{for } 6 < n < N. \end{aligned}$$

The first term of the left hand is equal to the $E_D(\mathcal{M}_i)$. Since the number of the rings in $\mathcal{R}_i^{n > 6}$ is constant independent of i , the second term bounded. Let C be the upper boundary of the sum of the Dirichlet energy of the rings in $\mathcal{R}_i^{n > 6}$, by Lemma 5.3.1, we finally obtain

$$(5.3.8) \quad E_D(\mathcal{M}_{i+1}) \leq E_D(\mathcal{M}_i) + \left(\lambda_1(N) - \frac{1}{2} \right) \lambda_1^{2i}(N) C.$$

When there are no n -rings with $n > 6$, then the inequality is strict for large enough i . The monotone increasing can be proved by the similar argument. \square

Chapter 6

Numerical Experiments and Applications

In this chapter, we provide the results of numerical experiments on both C_{60} and the Mackay crystal (Figure 6.1). Some of the results are included in the work collaborate with M. Kotani, H. Naito in [14]. In the numerical experiments, both the original GC-subdivision introduced in [37] and the modified method in Chapter 4 are discussed.

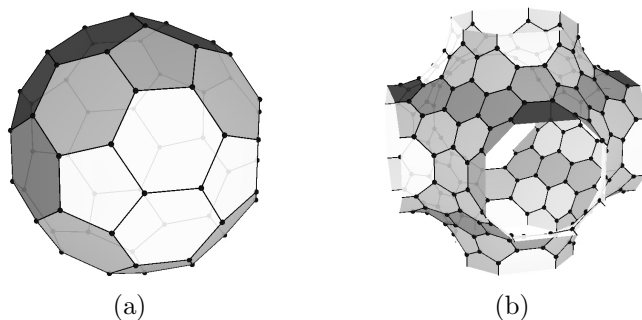


Figure 6.1: (a) C_{60} and (b) Mackay crystal of type P.

The C_{60} is the atomic structure of the famous fullerene. Each atom of the C_{60} has three bonds so that we can apply our method to study its subdivisions. Furthermore, the C_{60} is a carbon network on the sphere, which makes it a “positive curved” discrete surface. Also, each vertex of the C_{60} does not satisfy the balancing condition. These specific structures make the C_{60} a good example in our discrete surface theory.

On the other hand, the Mackay crystal is another carbon network. It is introduced by Mackay and Terrones [20] and studied as a triply periodic discrete minimal surface (Schwarz P surface). Opposite to the case of C_{60} , the Mackay crystal is a “negative curved” discrete surface and each of the vertices satisfies the balancing condition. In the work of M. Kotani, H. Naito and T. Omori [13], the Mackay crystal has been studied as a harmonic realization. They construct its subdivisions, however, do not give an explanation on the “topological defects” of the limit space. We provide a reason for this in the following.

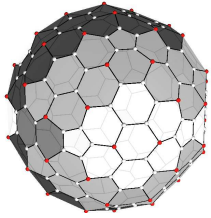
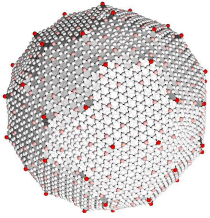
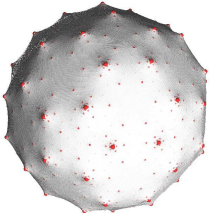
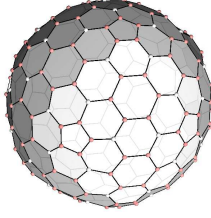

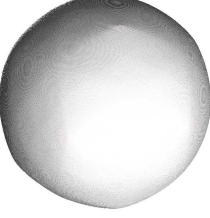
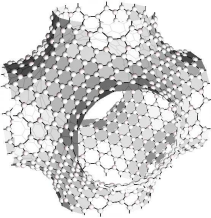
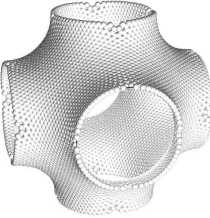
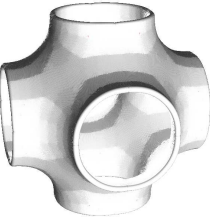
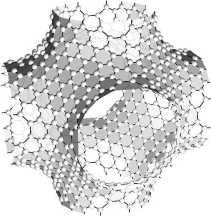
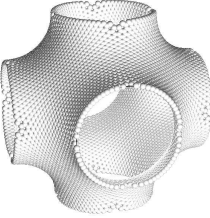
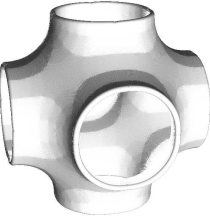
	1	3	6
Original method for C_{60}			
Modified method for C_{60}			
Original method for Mackay			
Modified method for Mackay			

Figure 6.2: Numerical computations of both the original and modified subdivision methods of C_{60} and Mackay crystal (the first, third, and sixth step). The color of each vertex is represented for the value of the corresponding height function. (Discussed in Chapter 2).

Figure 6.2 shows the results of numerical computations on the subdivisions of C_{60} and Mackay crystal. Both of the original subdivision method and the modified subdivision method are convergent. The first row of this figure shows that the vertices of the C_{60} and its subdivisions are performed as singularities when we apply the original subdivision method. However, the subdivisions of Mackay crystal generated by the original method produce few singularities (second row). This observation makes us consider the importance of the balancing condition. Thus we modify the original subdivision methods so that newly inserted vertices at each step satisfy the balancing conditions. The modified method provides a better result on the C_{60} also, a similar result on the Mackay crystal, as shown in the second row of this figure. On the other hand, in the third step of subdivisions of the Mackay crystal, one can easily find some “defects” at the boundaries which also appeared in [13]. These “defects” occurred at the accumulate points of the 8-rings. By Corollary 5.2.3, we can see the topological defects come from the difference of the convergent rates, which vary inversely with the size of the rings.

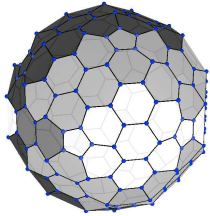
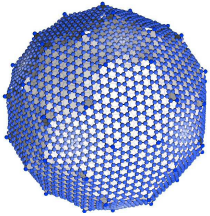
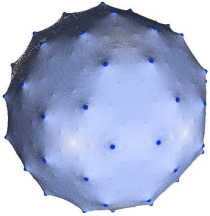
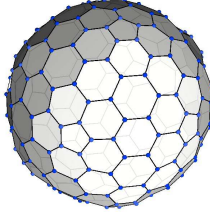
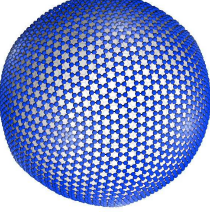
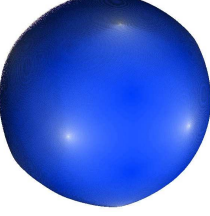
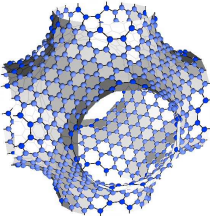
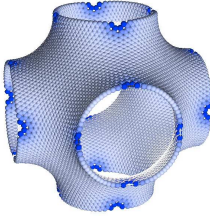
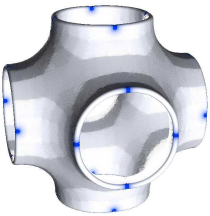
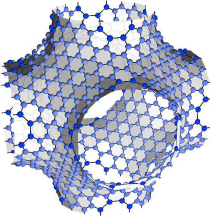
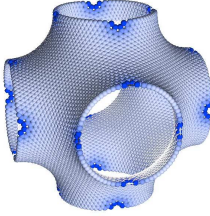
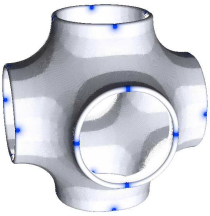
	1	3	6
Original method for C_{60}			
Modified method for C_{60}			
Original method for Mackay			
Modified method for Mackay			

Figure 6.3: Dirichlet energy of the subdivisions (the first, third, and sixth step). a) In the case of C_{60} , local energies around 5-rings are less than them around 6-rings while in the case of Mackay crystal, them around 8-rings are greater than them around 6-rings. b) In both cases, local energies around n -rings are greater than them around m -rings, if $n > m$. c) This observation is also confirmed in Figure 6.4, and supported by the calculations in Section 5.3.

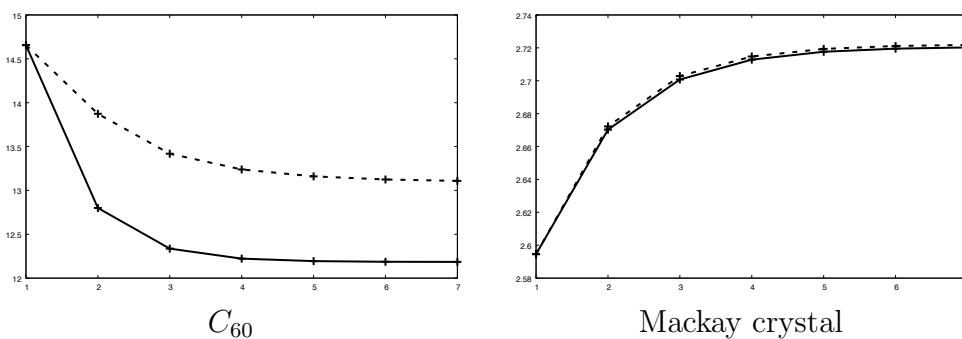


Figure 6.4: The Dirichlet energy of subdivisions of C_{60} and Mackay crystal. Dashed line: original subdivisions. Solid line: modified subdivisions.

Figure 6.3 and Figure 6.4 shows the Dirichlet energy of the subdivision sequences. We can see the Dirichlet energy of the subdivisions of C_{60} disperses at the 5-rings. However, the Dirichlet energy of the Mackay crystal concentrate at the 8-rings. By the Theorem 5.3.2, C_{60} has 6-rings and 5-rings then its energy monotonically decreases, while the Mackay has 6-rings and 8-rings so that the Dirichlet energy monotonically increases but bounded from above.

Bibliography

- [1] M. Alexa, M. Wardetzky Discrete laplacians on general polygonal meshes. *ACM Trans. Graph.*, **30**, 102, (2011). doi:10.1145/2010324.1964997.
- [2] A. I. Bobenko, H. Pottmann, and J. Wallner, A curvature theory for discrete surfaces based on mesh parallelity. *Math. Ann.*, **348**, 1–24, (2010). doi:10.1007/s00208-009-0467-9.
- [3] A. I. Bobenko and Y. B. Suris, Discrete differential geometry, volume 98 of *Graduate Studies in Mathematics*. American Mathematical Society, Providence, RI, 2008. doi:10.1007/978-3-7643-8621-4.
- [4] E. Catmull and J. Clark, Recursively generated B-spline surfaces on arbitrary topological meshes. *Comput. Aided Geom. Design*, **10**, 350–355, (1978). doi: 10.1016/0010-4485(78)90110-0.
- [5] O. Delgado-Friedrichs, Equilibrium placement of periodic graphs and convexity of plane tilings. *Discrete Comput. Geom.*, **33**, 67–81, (2005). doi:10.1007/s00454-004-1147-x.
- [6] M. Deza and M. Dutour Sikirić, Geometry of chemical graphs: polycycles and two-faced maps, volume 119 of *Encyclopedia of Mathematics and its Applications*. Cambridge University Press, Cambridge, 2008. doi:10.1017/CBO9780511721311.
- [7] D. Doo and M. Sabin, Behaviour of recursive division surfaces near extraordinary points. *Comput. Aided Geom. Design*, **10**, 356–360, (1978). doi: 10.1016/0010-4485(78)90111-2.
- [8] N. Dyn, D. Levine, and J. A. Gregory, A butterfly subdivision scheme for surface interpolation with tension control. *ACM Trans. Graph.*, **9**, 160–169, (1990). doi: 10.1145/78956.78958.
- [9] K. Hildebrandt, K. Polthier, and M. Wardetzky, On the convergence of metric and geometric properties of polyhedral surfaces. *Geom. Dedicata*, **123**, 89–112, (2006). doi:10.1007/s10711-006-9109-5.
- [10] K. Hildebrandt and K. Polthier Generalized shape operators on polyhedral surfaces. *Comput. Aided Geom. Design*, **28**, 321343, (2011). doi:10.1016/j.cagd.2011.05.001.
- [11] L. Kobbelt, Interpolatory subdivision on open quadrilateral nets with arbitrary topology. *Computer Graphics Forum*, **15**, 409–420, (1996). doi: 10.1111/1467-8659.1530409.

- [12] L. Kobbelt, $\sqrt{3}$ -Subdivision. *SIGGRAPH '00*, Proceedings of the 27th annual conference on Computer graphics and interactive techniques, 103–112, (2000). doi: 10.1145/344779.344835.
- [13] M. Kotani, H. Naito, and T. Omori, A discrete surface theory. *Comput. Aided Geom. Design*, **58**, 24–54, (2017). doi:10.1016/j.cagd.2017.09.002.
- [14] M. Kotani, H. Naito, and C. Tao, Construction of continuum from a discrete surface by its iterated subdivisions. *Communications in Analysis and Geometry*, (arXiv:1806.03531).
- [15] M. Kotani and T. Sunada, Large deviation and the tangent cone at infinity of a crystal lattice, *Math. Z.*, **254**, 837–870, (2006). doi:10.1007/s00209-006-0951-9.
- [16] M. Kotani and T. Sunada, Standard realizations of crystal lattices via harmonic maps. *Trans. Amer. Math. Soc.*, **353**, 1–20, (2001). doi:10.1090/S0002-9947-00-02632-5.
- [17] G. Li, W. Ma and H. Bao, $\sqrt{2}$ -subdivision for quadrilateral meshes. *Visual Computer*, **20**, 180–198, (2004). doi: 10.1007/s00371-003-0238-7.
- [18] C. Loop, Smooth subdivision surfaces based on triangles. *M.S. Mathematics thesis*, University of Utah, (1987).
- [19] C. Loop, Smooth ternary subdivision of triangle meshes. *Proceedings on Curves and Surfaces Fitting: Saint-Malo 2002*, 3–6, (2002). doi: 10.1.1.124.7010.
- [20] A. Mackay and H. Terrones. Diamond from graphite. *Nature*, **352**, 762, (1991). doi:10.1038/352762a0.
- [21] G. Morin, J. D. Warren and H. Weimer, A subdivision scheme for surfaces of revolution. *Comput. Aided Geom. Design*, **5**, 483–502, (2001). doi: 10.1016/S0167-8396(01)00043-7.
- [22] B. Oberknapp and K. Polthier, An algorithm for discrete constant mean curvature surfaces. *Visualization and mathematics (Berlin-Dahlem, 1995)*, 141–161. Springer, Berlin, 1997.
- [23] J. Peters and L. Shiue, Combining 4- and 3-direction subdivision. *ACM Trans. on Graph.*, **23**, 980–1003, (2004). doi: 10.1145/1027411.1027415.
- [24] U. Pinkall and K. Polthier, Computing discrete minimal surfaces and their conjugates. *Experiment. Math.*, **2**, 15–36, (1993). <http://projecteuclid.org/euclid.em/1062620735>.
- [25] K. Polthier Computational aspects of discrete minimal surfaces. *Clay Math. Proc.*, **2**, 65–111, (2005).
- [26] K. Polthier and W. Rossman, Discrete constant mean curvature surfaces and their index. *J. Reine Angew. Math.*, **549**, 47–77, (2002). doi:10.1515/crll.2002.066.
- [27] K. Polthier and E. Preuß, Identifying vector field singularities using a discrete Hodge decomposition. *Visualization and mathematics*, **III**, 113–134, (2003).

- [28] K. Polthier and M. Schmies, Straightest geodesics on polyhedral surfaces. *Mathematical visualization*, 135–150, (1998).
- [29] H. Prautzsch, Freeform splines. *Comput. Aided Geom. Design*, **9**, 377–390, (1997). doi: 10.1016/S0167-8396(96)00029-5.
- [30] U. Reif, A unified approach to subdivision algorithms near extraordinary vertices. *Comput. Aided Geom. Design*, **12**, 153–174, (1995). doi: 10.1016/0167-8396(94)00007-F.
- [31] U. Reif, TURBS–Topologically unrestricted rational B-splines. *Constructive Approximation*, **14**, 57–77, (1998).
- [32] U. Reif and J. Peters, The simplest subdivision scheme for smoothing polyhedra. *ACM Trans. Graph.*, **16**, 420–431, (1998).
- [33] D. E. Smith, *A source book in mathematics*. 2 vols. Dover Publications, Inc., New York 1959.
- [34] J. Stam Exact evaluation of Catmull-Clark subdivision surfaces at arbitrary parameter values. *Proceedings of the 25th annual conference on computer graphics and interactive techniques*, SIGGRAPH’98, 395–404, (1998).
- [35] J. Stam and C. Loop Quad/triangle subdivision. *Computer Graphics Forum*, **22**, 79–86, (2003). doi: 10.1111/1467-8659.t01-2-00647.
- [36] T. Sunada, Crystals that nature might miss creating. *Notices Amer. Math. Soc.*, **55**, 208–215, (2008).
- [37] C. Tao, A construction of converging Goldberg-Coxeter subdivisions of a discrete surface. *Kobe Journal of Mathematics*, submitted.
- [38] L. Velho and D. Zorin 4–8 Subdivision. *Comput. Aided Geom. Design*, **18**, 397–427, (2001). doi: 10.1016/S0167-8396(01)00039-5.